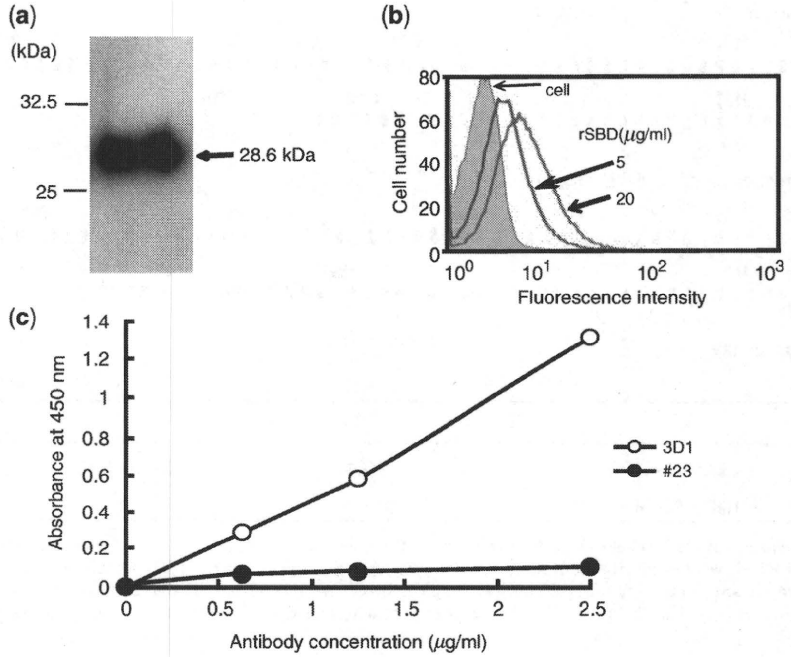

Fig. 7 H5 sugar-binding domain (H5 rSBD) recognized with 3D1 scFv. (a) SDS–PAGE analysis of His-tag-colum-fractionated H5 rSBD protein. The H5 rSBD protein was electrophoresed in 12.5% gel under reducing conditions. The H5 rSBD protein was blotted onto a PVDF membrane, blocked with 5% skim milk, and probed with anti-His-tag mAb. (b) Flow cytometry analysis was performed with MDCK cells. Cells were incubated with rSBD at the concentrations of 5 and 20 μg/ml. The concentration was estimated as described earlier (*20*). rSBD binding was monitored with mouse anti-His-tag mAb and FITC-anti mouse IgG mAb. (c) rSBD-binding activity of 3D1 scFv by ELISA. Microtiter plates were pre-coated with a serial concentration of scFv antibody, ranging from 2.5 to 0.8 μg/ml, followed by the addition of 3 μg/ml of rSBD. The binding of H5 rSBD to scFv antibody was detected by using mouse anti-His-tag mAb and HRP-conjugated anti mouse IgG mAb. ELISA was performed as described in Fig. 3.

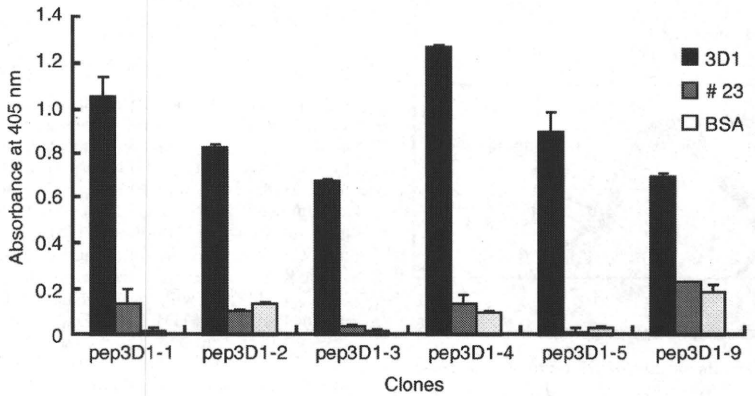

Fig. 8 Epitope analysis: Ph.D-12 clones specifically bound to 3D1 scFv: 3D1 scFv-specific peptide-displaying phage clones were isolated from peptide-displaying phage library (Ph.D-12). The ELISA plate was coated with 3D1 or #23 scFv (100 ng/50 μl). The phage clones (5.0×10^{10} virions/50 μl) were added to the wells, and their binding was detected by a biotinylated anti-M13 mAb in combination with AP-conjugated streptavidin.

#128-131 in the case of pep3D1-1) while pep3D1-9 sequence motif showed weak homology at the regions splitted at #287-293 and #367-368 of H5 HA molecule of A/Vietnam/1194/2004 influenza virus strain (Fig. 9a). The H5 HA structure was depicted according to the PyMoL (molecular visualization system) using a database of the PDB code, 2IBX, as shown in Fig. 9b. These regions correspond to the 190-helix and 130-loop of H5 HA, which have been reported as regions responsible for binding sites to sialic acid α2, 6-galactose (SA α2,6Gal) or sialic acid α2, 3-galactose (SA α2,3Gal) (*32*).

Discussion

In the present study, we established a human anti-H5 scFv, 3D1, by biopanning with recombinant H5-Fc from a naïve scFv-displaying phage library.

(a)

Virus or clone name	Amino acid sequence	Frequence
	121 131 141 151 161 171 181 191 201 211	
H5 (VN1194)	HFEKIQIIPKSSWSSHEASLGVSSACPYQGKSSFFRNVVWLIKKNSTYPTIKRSYNNTNQEDLLVLWGIHHPKDAAEQTKLYQNPTTYISVGTS	
pep3D1-1	- - - -LPSS- SPTPFLSG- - :*.* .**.::*	5/6

(b)

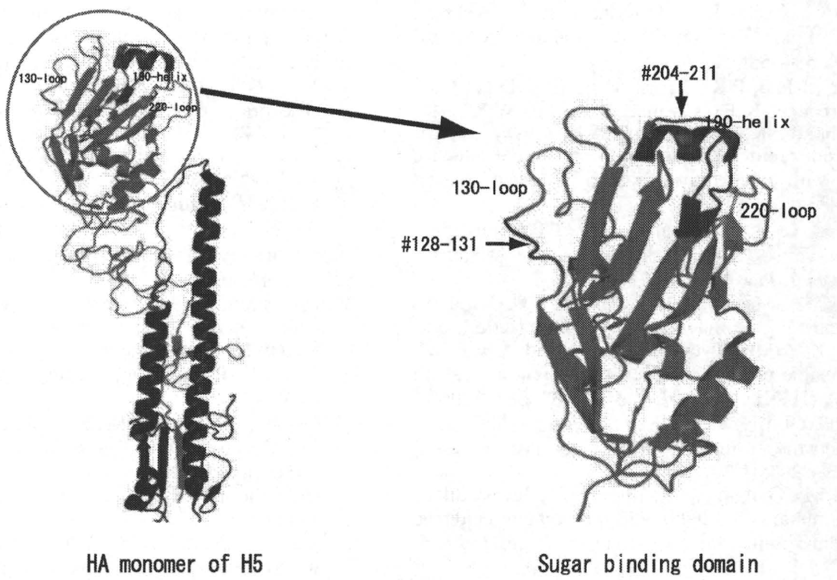

Fig. 9 Major epitope of 3D1 scFv locates at the H5 sugar-binding region. (a) A major epitope of 3D1 scFv, pep3D1-1 is analysed on the homologous region with H5 HA using CLUSTAL W ver. 3.1. The mark, 'asterisk', 'colon' or 'dot', indicated below the epitope sequence, indicates identical, conserved or semi-conserved residues, respectively. The weakly homologous regions correspond to the 190-helix and 130-loop of H5 HA. (b) Magnified picture of the globular head of H5. The H5 hemagglutinin structure was depicted according to the PyMoL (molecular visualization system) using a database of the PDB code, 2IBX. The binding site comprises three structure elements: an 1-helix (190-helix) and 2-loops (130-loop and 220-loop), which have been reported as regions responsible for binding sites to sialic acid α2,6-galactose (SA α2,6Gal) or sialic acid α2,3-galactose (SA α2,3Gal) (*32*). The epitope regions of 3D1 scFv are depicted in red (#204-211 and #128-131).

3D1 showed a neutralizing activity (Fig. 6) even if it was scFv and was purified as a monovalent form by gel permeation chromatography (Fig. 2). To investigate the binding epitope of 3D1, the specific binding clones to 3D1 from a peptide-display phage library (Ph.D-12) were selected, and their binding peptide sequences were determined. Homology analysis of CLUSTAL W showed that the major epitope sequences were weakly homologous to #204-211 and #128-131 of H5 HA of the A/Vietnam/1194/2004 influenza virus strain. These regions correspond to the 190-helix and 130-loop of H5 HA, which have been reported as the regions responsible for binding sites to sialic acid α2,6-galactose (SA α2,6Gal) or sialic acid α2,3-galactose (SA α2,3Gal) from comparative analyses of the amino acid sequences of varying H5N1 isolates (A/Vietnam/1194/2004) (*32*). This finding suggests that 3D1 might recognize the conformation structure but not the linear epitope of the sugar-binding domain of H5. We demonstrated a consistent result in which 3D1 bound to the rSBD (#50G-#272E) produced by the baculovirus vector system.

Although human anti-H5 scFvs or Fab antibodies with cross-clade reactivities have been reported (*28*, *33–35*), their binding epitopes have not been determined. Anti-H5 antibodies reactive to either the conserved region of HA2 or the conserved pocket in the stem region of H5 HA have also been reported.

However, as 3D1 is the first human scFv of which the mimotope has been defined on the sugar-binding epitope, it is possible to identify the amino acids contributing the fine binding specificity in this region by amino-acid substitution experiments. Furthermore, 3D1 antibody may be useful for passive immunization against H5N1 virus infection.

Conflict of interest

None declared.

References

1. Cannell, J.J., Zasloff, M., Garland, C.F., Scragg, R., and Giovannucci, E. (2008) On the epidemiology of influenza. *J. Virol.* **5**, 29–41
2. Michaelis, M., Doerr, H.W., and Cinatl, J. (2009) Novel swine-origin influenza A virus in humans: another pandemic knocking at the door. *Med. Microbiol. Immunol.* **198**, 175–183

3. Neumann, G., Noda, T., and Kawaoka, Y. (2009) Emergence and pandemic potential of swine-origin H1N1 influenza virus. *Nature* **459**, 931–939
4. Claas, E.C., Osterhaus, A.D., van-Beek, R., De-Jong, J.C., Rimmelzwaan, G.F., Senne, D.A., Krauss, S., Shortridge, K.F., and Webster, R.G. (1998) Human influenza A H5N1 virus related to a highly pathogenic avian influenza virus. *Lancet* **351**, 472–477
5. de-Jong, J.C., Claas, E.C., Osterhaus, A.D., Webster, R.G., and Lim, W.L. (1997) A pandemic warning? *Nature* **389**, 554–555
6. Yuen, K.Y., Chan, P.K., Peiris, M., Tsang, D.N., Que, T.L., Shortridge, K.F., Cheung, P.T., To, W.K., Ho, E.T., Subbarao, K., and Cheng, A.F. (1998) Clinical features and rapid viral diagnosis of human disease associated with avian influenza A H5N1 virus. *Lancet* **351**, 467–471
7. Gillim-Ross, L. and Subbarao, K. (2006) Emerging respiratory viruses: challenges and vaccine strategies. *Clin. Microbiol. Rev.* **19**, 614–636
8. Ungchusak, K., Auewarakul, P., Dowell, S.F., Kitphati, R., Auwanit, W., Puthavathana, P., Uiprasertkul, M., Boonnak, K., Pittayawonganon, C., and Cox, N.J. (2005) Probable person-to-person transmission of avian influenza A (H5N1). *N. Engl. J. Med.* **352**, 333–340
9. WHO. (2008) http://www.who.int/csr/disease/influenza/influenzanetwork/en/index.htmlS (date last accessed 16 December 2008)
10. Hoelscher, M., Gangappa, S., Zhong, W., Jayashankar, L., and Sambhara, S. (2008) Vaccines against epidemic and pandemic influenza. *Expert. Opin. Drug. Deliv.* **5**, 1139–1157
11. Tambyah, P.A. (2008) Update on influenza vaccines. *Respirology* **13**, 41–43
12. de Jong, M.D., Simmons, C.P., Thanh, T.T., Hien, V.M., Smith, G.J., Chau, D.M., Hoang, N.V., Chau, T.H., Khanh, V.C., Dong, P.T., Qui, B.V., Cam, D.Q., Ha, Y., Guan, J.S., Peiris, N.T., Chinh, T.T., and Farrar, J. (2006) Fatal outcome of human influenza A (H5N1) is associated with high viral load and hypercytokinemia. *Nat. Med.* **12**, 1203–1207
13. Simmons, C.P., Bernasconi, N.L., Suguitan-Jr, A.L., Mills, K., Ward, J.M., Chau, N.V.V., Hien, T.T., Sallusto, F., Ha-do, Q., Farrar, J., de Jong, M.D., Lanzavecchia, A., and Subbarao, K. (2007) Prophylactic and therapeutic efficacy of human monoclonal antibodies against H5N1 influenza. *PLoS. Med.* **4**, e178–e187
14. Hanson, B.J., Boon, A.C., Lim, A.P., Webb, A., Ooi, E.E., and Webby, R.J. (2006) Passive immunoprophylaxis and therapy with humanized monoclonal antibody specific for influenza A H5 hemagglutinin in mice. *Respir. Res.* **7**, 126–136
15. Kashyap, A.K, Steel, J., Oner, A.F., Dillon, M.A., Swale, R.E., Wall, K.M., Perry, K.J., Faynboym, A., Ilhan, M., Horowitz, M., Horowitz, L., Palese, P., Bhatt, R.R., and Lerner, R.A. (2008) Combinatorial antibody libraries from survivors of the Turkish H5N1 avian influenza outbreak reveal virus neutralization strategies. *Proc. Natl Acad. Sci. USA* **105**, 5986–5991
16. Abdel-Ghafar, A.N., Chotpitayasunondh, T., Gao, Z., Hayden, F.G., Nguyen, D.H., de Jong, M.D., Naghdaliyev, A., Peiris, J.S., Shindo, N., Soeroso, S., and Uyeki, T.M. Writing Committee of the Second World Health Organization Consultation on Clinical Aspects of Human Infection with Avian Influenza A (H5N1) Virus. (2008) Update on avian influenza A (H5N1) virus infection in humans. *N. Engl. J. Med.* **358**, 261–273
17. Hoogenboom, H.R. (2005) Selecting and screening recombinant antibody libraries. *Nat. Biotechnol.* **23**, 1105–1116
18. Benhar, I. (2007) Design of synthetic antibody libraries. *Expert Opin. Biol. Ther.* **7**, 763–779
19. Takada, A., Matsushita, S., Ninomiya, A., Kawaoka, Y., and Kida, H. (2003) Intranasal immunization with formalin-inactivated virus vaccine induces a broad spectrum of heterosubtypic immunity against influenza A virus infection in mice. *Vaccine* **21**, 3212–3218
20. Pace, C.N., Vajdos, F., Fee, L., Grimsley, G., and Gray, T. (1995) How to measure and predict the molar absorption coefficient of a protein. *Protein Sci.* **4**, 2411–2423
21. Hashiguchi, S., Nakashima, T., Nitani, A., Yoshihara, T., Yoshinaga, K., Ito, Y., Maeda, Y., and Sugimura, K. (2003) Human Fc epsilon RIalpha-specific human single-chain Fv (scFv) antibody with antagonistic activity toward IgE/Fc epsilon RIalpha-binding. *J. Biochem.* **133**, 43–49
22. Hamasaki, T., Hashiguchi, S., Ito, Y., Nakanishi, K., Nakashima, T., and Sugimura, K. (2005) Human anti-human IL-18 antibody recognizing the IL-18-binding site 3 with IL-18 signaling blocking activity. *J. Biochem.* **138**, 433–442
23. Gejima, R., Tanaka, K., Nakashima, T., Hashiguchi, S., Ito, Y., Yoshizaki, K., and Sugimura, K. (2002) Human single-chain Fv (scFv) antibody specific to human IL-6 with the inhibitory activity on IL-6-signaling. *Hum. Antibodies* **11**, 121–129
24. Kaji, M., Ikari, M., Hashiguchi, S., Ito, Y., Matsumoto, R., Yoshimura, T., Kuratsu, J., and Sugimura, K. (2001) Peptide mimics of monocyte chemoattractant protein-1 (MCP-1) with an antagonistic activity. *J. Biochem.* **129**, 577–583
25. Hashimoto, T., Wakabayashi, T., Watanabe, A., Takio, K., Mann, D.M., and Iwatsubo, T. (2002) CLAC: a novel Alzheimer amyloid plaque component derived from a transmembrane precursor, CLAC-P/collagen type XXV. *EMBO J.* **21**, 1524–1534
26. Kabat, E.A. and Wu, T.T. (1991) Identical V region amino acid sequences and segments of sequences in antibodies of different specificities. Relative contributions of VH and VL genes, minigenes, and complementarity-determining regions to binding of antibody combining sites. *J. Immunol.* **147**, 1709–1719
27. Johnson, G., Wu, T. T., and Kabat, E. A. (1995) SEQHUNT. A program to screen aligned nucleotide and amino acid sequences. *Methods Mol. Biol.* **51**, 1–15
28. Sui, J., Hwang, W.C., Perez, S., Wei, G., Aird, D., Chenn, L., Santelli, E., Stec, B., Cadwell, Greg., Ali, M., Wan, H., Murakami, A., Yammanuru, A., Han, T., Cox, N.J., Bankaton, L.A., Donis, R.O., Liddinqton, R.C., and Marasco, W.A. (2009) Structural and functional bases for broad-spectrum neutralization of avian and human influenza A viruses. *Nat. Struct. Mol. Biol.* **16**, 265–273
29. WHO. (2007) http://www.who.int/csr/disease/avian_influenza/guidelines/summaryH520070403.pdf
30. WHO. (2005) Evolution of H5N1 avian influenza viruses in Asia. *Emerg. Infect. Dis.* **11**, 1515–1521
31. Broxhet, X., Lefranc, M. P., and Giudicelli, V. (2008) IMGT/V-QUEST: the highly customized and integrated system for IG and TR standardized V-J and V-D-J sequence analysis. *Nucleic Acids Res.* **36**, W503–W508
32. Stevens, J., Blixt, O., Tumpey, T.M., Taubenberger, J.K., Paulson, J.C., and Wilson, I.A. (2006) Structure and receptor specificity of the hemagglutinin from an H5N1 influenza virus. *Science* **312**, 404–410

33. Lim, A.P., Chan, C.E., Wong, S.K., Chan, A.H., Ooj, E.E., and Hanson, B.J. (2008) Neutralizing human monoclonal antibody against H5N1 influenza HA selected from a Fan-phage display library. *J. Virol.* **5**, 130–140
34. Maneewatch, S., Thanongsaksrikul, J., Songserm, T., Thueng-In, K., Kulkeaw, K., Thathaisong, U., Srimanote, P., Tongtawe, P., Tapchaisri, P., and Chaicumpa, W. (2009) Human single-chain antibodies that neutralize homologous and heterologous strains and clades of influenza A virus subtype H5N1. *Antivir. Ther.* **14**, 221–230
35. Ascione, A., Capecchi, B., Campitelli, L., Imperiale, V., Flego, M., Zamboni, S., Gellini, M., Alberini, I., Pittiglio, E., Donatelli, I., Temperton, N.J., and Cianfriglia, M. (2009) Human monoclonal antibodies in single chain fragment variable format with potent neutralization activity against influenza virus H5N1. *Antiviral Res.* **83**, 238–244

ARTICLE

Journal of Cellular Biochemistry 111:461–468 (2010)

Journal of Cellular Biochemistry

Multiple Mechanisms for Exogenous Heparin Modulation of Vascular Endothelial Growth Factor Activity

Errol Wijelath,[1*] Mayumi Namekata,[1] Jacqueline Murray,[1] Mai Furuyashiki,[2] Siyuan Zhang,[3] Daniel Coan,[1] Masahiro Wakao,[4] Robert B. Harris,[5] Yasuo Suda,[2,4] Lianchun Wang,[3] and Michael Sobel[1]

[1]*Department of Surgery, Division of Vascular Surgery, VA Puget Sound Health Care System and the University of Washington School of Medicine, Seattle, Washington*

[2]*SUDx-Biotec Corporation, Kobe, Japan*

[3]*Department of Biochemistry and Molecular Biology, Complex Carbohydrate Research Center, University of Georgia, Athens, Georgia*

[4]*Department of Nanostructure and Advanced Materials, Graduate School of Science and Engineering, Kagoshima University, Kagoshima, Japan*

[5]*Commonwealth Biotechnologies, Inc., Richmond, Virginia*

ABSTRACT

Heparin and heparin-like molecules are known to modulate the cellular responses to vascular endothelial growth factor-A (VEGF-A). In this study, we investigated the likely mechanisms for heparin's influence on the biological activity of VEGF-A. Previous studies have shown that exogenous heparin's effects on the biological activity of VEGF-A are many and varied, in part due to the endogenous cell-surface heparan sulfates. To circumvent this problem, we used mutant endothelial cells lacking cell-surface heparan sulfates. We showed that VEGF-induced cellular responses are dependent in part on the presence of the heparan sulfates, and that exogenous heparin significantly augments VEGF's cellular effects especially when endogenous heparan sulfates are absent. Exogenous heparin was also found to play a cross-bridging role between VEGF-A_{165} and putative heparin-binding sites within its cognate receptor, VEGFR2 when they were examined in isolation. The cross-bridging appears to be more dependent on molecular weight than on a specific heparin structure. This was confirmed by surface plasmon resonance binding studies using sugar chips immobilized with defined oligosaccharide structures, which showed that VEGF-A_{165} binds to a relatively broad range of sulfated glycosaminoglycan structures. Finally, studies of the far-UV circular dichroism spectra of VEGF-A_{165} showed that heparin can also modulate the conformation and secondary structure of the protein. J. Cell. Biochem. 111: 461–468, 2010. © 2010 Wiley-Liss, Inc.

KEY WORDS: VEGF-A; VEGFR2; HEPARIN; ENDOTHELIAL CELL; Ndst

Vascular endothelial growth factor-A (VEGF-A), a secreted glycoprotein, plays a key role in regulating both normal and pathological angiogenic processes [Dvorak, 2005]. The importance of VEGF-A in vascular development was demonstrated in mouse models showing that loss of even a single VEGF-A allele results in lethal vascular defects [Carmeliet et al., 1996]. The main function of VEGF-A is to promote endothelial cell proliferation, migration and survival [Ferrara et al., 2003]. The most abundant spliced variant form of VEGF-A is VEGF-A_{165}, which contains a heparin binding domain encoded by exons 6 and 7 [Tischer et al., 1991]. Heparins and heparan sulfates are known to have pleiomorphic effects on the biological actions of VEGF-A [Neufeld et al., 1999]. However, the elucidation of heparin's effects and mechanisms of actions are complicated by the multiplicity of potential heparin-binding partners involved. Not only does VEGF-A_{165} bind heparin, but so do its principal receptor, VEGFR2, as well as VEGFR1 and neurophilin, a co-receptor for VEGF-A [Dougher et al., 1997; Soker et al., 1998; Park and Lee, 1999]. Furthermore, endothelial cells

Grant sponsor: NIH; Grant numbers: RO1HL097182, P41RR005351; Grant sponsor: Japan Science and Technology Agency.

*Correspondence to: Dr. Errol Wijelath, PhD, Department of Surgery, Division of Vascular Surgery, VA Puget Sound Health Care System, S151, 1660, S Columbian Way, Seattle, WA 98108. E-mail: errolw@u.washington.edu

Received 12 February 2010; Accepted 28 May 2010 • DOI 10.1002/jcb.22727 • © 2010 Wiley-Liss, Inc.
Published online 3 June 2010 in Wiley Online Library (wileyonlinelibrary.com).

present other heparin-binding sites on their cell surface, including the heparan sulfate proteoglycans (HSPG) [Neufeld et al., 1999]. Exogenous heparin potentiates the binding of VEGF-A to endothelial cells and promotes endothelial cell proliferation, migration and tube formation [Gitay-Goren et al., 1992; Ono et al., 1999; Ashikari-Hada et al., 2005; Lake et al., 2006]. However, most studies of this phenomenon have employed chlorate or heparinase treatments of endothelial cells, which may have unforeseen effects on cellular responses. This present study was undertaken to elucidate the range of influences of heparin on VEGF-A activity, beginning with an endothelial cell line that constitutively lacks sulfation of the cell-surface heparan sulfates, continuing with studies of heparin modulation of VEGF-receptor binding in cell-free systems, and concluding with an examination of the influence of glycosaminoglycan structure on VEGF-A binding and protein conformation.

MATERIALS AND METHODS

VEGF PROTEIN

VEGF-A_{165} was a gift from Genetech. VEGF-A_{121} was expressed in *Pichia pastoris* as described by the manufacturer (Invitrogen).

HEPARINS

Throughout our experiments we employed a standard unfractionated porcine mucosal heparin (molecular weight ~15,000 Da) that has been thoroughly characterized (Celsus, Inc.). For SPR experiments, low molecular weight heparins (LMWH) were prepared by periodate/alkali treatment of a comparable porcine heparin (Nacalai Tesque, Kyoto, Japan), and by fractionation according to their molecular weight as we have previously described [Suda et al., 1993]. For circular dichroism, a LMWH ~5,000 Da was purchased from Calbiochem and a high molecular weight heparin of ~21,000 Da was prepared, as previously described, by affinity fractionation of the standard unfractionated heparin, using a heparin-binding peptide [Poletti et al., 1997].

ENDOTHELIAL CELL LINES

$Ndst2^{-}/^{-}$ and its daughter $Ndst1^{-/-}$ $Ndst2^{-/-}$ mouse lung endothelial cells were generated as previously described [Wang et al., 2005]. In this current study, we utilized these two mutant endothelial cell lines and also a newly generated $Ndst1^{+}/^{+}Ndst2^{+}/^{+}$ line as wild-type control which was similarly derived from wild-type mice. All three endothelial cell lines were derived from fully backcrossed C57Bl/6J mice and possess the same genetic background.

FLOW CYTOMETRY ANALYSIS OF GLYCOSAMINOGLYCAN AND GROWTH FACTOR BINDING TO ENDOTHELIAL CELLS LACKING NDST ENZYMES

Endothelial cells (80% confluent) were harvested with 2 mM EDTA containing 0.1% BSA in PBS (PBS-B-E buffer) and incubated with mouse IgM type anti-CS antibody (1:200, Sigma) or anti-heparan sulfate antibody (10E4, 1:500, Seikagaku) respectively for 1 h with shaking at 4°C. Normal mouse IgM staining served as background control. For basic fibroblast growth factor (FGF-2) binding studies, harvested endothelial cells were incubated with 0.6 μg/ml biotinlyated-FGF-2 in PBS-B-E buffer on ice for 30 min. To detect cell surface VEGF binding, endothelial cells were incubated for 1 h at 4°C with recombinant human biotinylated $VEGF_{165}$ (1.1 μg/ml in PBS; R&D Systems). As controls, the same cells were incubated with an irrelevant biotinylated protein (soybean trypsin inhibitor) (Invitrogen; 8 μg/ml for 45 min at 4°C). Cells were then washed with PBS-B-E buffer and incubated with FITC-conjugated goat anti-mouse IgM (for anti-HS and anti-CS antibody, 1:1000, Invitrogen) for 1 h or with FITC-streptavidin (1:1,000, Pierce) for 15 min on ice. Thereafter, the cells were washed twice with PBS-B-E buffer and analyzed by Cell Lab Quanta SC flow cytometer (Beckman Coulter). Twenty thousand cell counts were collected and analyzed by the FlowJo software (Tree Star, Inc.).

MEASUREMENT OF ERK AND VEGFR2 PHOSPHORYLATION

Preliminary experiments established that 5 ng/ml was the concentration for VEGF-A that activated Erk and VEGFR2 that was below the saturation point. This concentration of VEGF-A allowed us to analyzed the change in the phosphorylation state of Erk and VEGFR2 in the presence of heparin. Detection and analysis of Erk and VEGFR2 phosphorylation were performed as described previously [Wijelath et al., 2006]. Signal densities from Western blots were quantified using the NIH Image program, and the results of three or more independent experiments pooled for analysis. Activated Erk and VEGFR2 were expressed as fold increase in phosphorylation over basal (unstimulated) levels.

SURFACE PLASMON RESONANCE BINDING STUDIES

Surface plasmon resonance (SPR) experiments were performed with an SPR-670 M (Moritex, Yokohama, Japan) under the manufacturer's recommended guidelines with slight modifications [Wakao et al., 2008]. Two different approaches were taken. First, heparin modulation of VEGF-165 binding to its receptor VEGFR2 was measured. VEGFR2-Fc protein was immobilized on protein A-coated gold sensor chips. The carboxyl groups immobilized chips were purchased from SUDx-Biotec (Kagoshima, Japan) and were activated for 15 min with a mixture of 0.2 M 1-ethyl-3-(3-dimethylaminopropyl)-carbodiimide (EDC) and 0.05 M *N*-hydroxysuccinimide in 90% dioxane. With continuous monitoring of resonance units, Protein A was immobilized to the activated chip by injecting 2 × 100 μl (100 μg/ml) in PBS pH 6. Excess reactive groups were quenched with 1 M ethanolamine-HCl, pH 8.5. VEGFR2-Fc (10 μg/ml) was then immobilized to protein A by injecting 2 × 100 μl in PBS. A flow cell without immobilized VEGFR2-Fc served as the negative control. For binding studies, VEGF-A was injected into the flow cells in PBS containing 0.05% Tween-20 (PBST) with or without heparin. VEGF-A/heparin mixtures were pre-incubated for 10 min at room-temperature before injection into the flow cell. Sensor chips were regenerated by treating with 1.5 M glycine/NaOH, 3 M NaCl, pH 9.

For the second approach, a novel "sugar chip" technology was used to measure the affinity of VEGF-A for a library of different, defined oligosaccharide structures. The array type sugar chips (GAG-chips) were supplied from SUDx-Biotec as previously described [Suda et al., 2006]. Totally synthetic, defined disaccharide

structures derived from heparin and related glycosaminoglycans, as well as positive and negative controls (12 in all) were immobilized on the chips of SPR imaging apparatus (SPRinter, Toyobo, Osaka, Japan). The solvent for the binding experiments was PBST at pH 7.4, run at a flow rate of 15 μl/min at 25°C containing a range of concentrations of VEGF-A (12–400 nM) and heparin. Binding was recorded as resonance units, and the kinetic binding parameters deconvoluted using the manufacturer's software to calculate on- and off-rates and dissociation constants.

CIRCULAR DICHROISM

The far-UV circular dichroism spectra of VEGF-A_{165} and VEGF-A_{121} protein were measured in a Jasco Model 715 Spectropolarimeter equipped with a Jasco Model PTC-348WI Peltier temperature controller. The system is operated by Jasco Hardware Manager (ver. 1.50.00) and data collected by Jasco J-700 Analysis Software (ver. 1.50.01). Protein samples were assayed at 2.78 μM (0.1 mg/ml) VEGF-A. A measured volume of 200 μl of protein was placed in a cell with a 0.1 cm light path length, thermostatted at 20°C. The samples were scanned from 350 to 170 nm at a scan speed of 100 nm/min, and two spectra were accumulated for each sample. Circular dichroism spectra were measured for the protein alone, and after the sequential addition of 0.5 μM increments of unfractionated heparin. Spectral data were analyzed for secondary structure using Dicroprot (ver 2.4).

RESULTS

HEPARAN SULFATION IS MARKEDLY REDUCED IN NDST1/2-NULL CELLS

To clarify the role of HSPG, particularly their sulfated moieties, we studied the effects of heparins and VEGF-A on mutant strains of mouse endothelial cells that naturally lacked sulfated heparans. We first analyzed the degree of sulfation on $Ndst1^{+/+}Ndst2^{+/+}$ (wild-type), $Ndst1^{+/+}Ndst2^{-/-}$, and $Ndst1^{-/-}Ndst2^{-/-}$ endothelial cell lines using an anti-heparan sulfate antibody 10E4. Ablation of both Ndst1 and Ndst2 attenuates cell surface 10E4 binding by more than 80% whereas Ndst2 ablation does not alter endothelial cell surface heparan sulfate structure, when compared to $Ndst1^{+/+}Ndst2^{+/+}$ mouse endothelial cells (Fig. 1A). The residual 20% binding of $Ndst1^{-/-}Ndst2^{-/-}$ cells may reflect the binding of the antibody to the *N*-acetylated glucosamine structure of heparan sulfate since the 10E4 antibody recognizes both *N*-sulfated and *N*-acetylated structures of heparan sulfate. To confirm the reduced sulfation of the $Ndst1/2^{-/-}$ endothelial cell surface heparan sulfate, we analyzed the binding of FGF-2 since FGF-2 binding to cell surface heparan sulfate is critically dependent on *N*- and 2-*O*-sulfation. Simultaneous ablation of Ndst1 and Ndst2 attenuated cell surface FGF-2 binding by more than 90% (Fig. 1B). However, Ndst2 ablation alone did not alter endothelial cell surface FGF-2 binding. To determine whether the Ndst1/2 ablation alters cell surface chondroitin sulfates (CS) expression, the mutant cells were stained with anti-CS antibody. Cell surface CS levels were similar among $Ndst1^{+/+}Ndst2^{+/+}$, $Ndst1^{+/+}Ndst2^{-/-}$ and $Ndst1^{-/-}Ndst2^{-/-}$ endothelial cells, demonstrating that Ndst ablation did not affect CS expression (Fig. 1C). We next examined the binding of VEGF-A on these cell-lines. Cell surface VEGF-A binding analysis showed that, although Ndst2 ablation does not alter endothelial cell surface VEGF-A binding, the simultaneous ablation of Ndst1 and Ndst2 attenuated cell surface VEGF-A binding by about 85% (Fig. 1D). The residual 15% cell surface VEGF-A binding may reflect low affinity binding to VEGFR2. Taken together, these cell surface profiles illustrate that the $Ndst1^{+/+}Ndst2^{-/-}$ endothelial heparan sulfate possesses normal heparan sulfate structure, whereas the $Ndst1^{-/-}Ndst2^{-/-}$ endothelial heparan sulfates have very low or no sulfates. CS expression was unaffected in all cell lines.

ACTIVATION OF ERK AND VEGFR2

As shown above, the $Ndst1^{+/+}Ndst2^{-/-}$ and the $Ndst1^{-/-}Ndst2^{-/-}$ endothelial cell lines are suitable cell-systems to examine the requirement of endogenous heparan sulfates and also the role of exogenous heparin for VEGF-A signaling. $Ndst1^{+/+}Ndst2^{+/+}$, $Ndst1^{+/+}Ndst2^{-/-}$ and $Ndst1^{-/-}Ndst2^{-/-}$ mouse endothelial cell cultures were simultaneously exposed to VEGF-A (5 ng/ml) and different concentrations of unfractionated heparin (1–50 μg/ml). Erk phosphorylation was measured after 5 min. Figure 2 illustrates the results of three independent experiments. VEGF alone modestly increased Erk phosphorylation in all three cell lines. Increasing concentrations of exogenous heparin steadily increased Erk phosphorylation induced by VEGF-A (Fig. 2A). However, cells lacking endogenous heparan sulfates ($Ndst1^{-/-}Ndst2^{-/-}$) responded much more dramatically to exogenous heparin, far exceeding the increase in Erk induced by heparin/VEGF-A in the $Ndst1^{+/+}Ndst2^{+/+}$ and $Ndst1^{+/+}Ndst2^{-/-}$ cells at 10 μg/ml of heparin only ($P < 0.01$, *t*-test). We then investigated how exogenous heparin would influence VEGF's interaction with its principle cognate receptor, VEGFR2. Figure 2B shows that the pattern of VEGFR2 responses to heparin/VEGF was quite similar to the Erk responses. The $Ndst1^{-/-}Ndst2^{-/-}$ cells deficient in sulfated heparans induced more VEGFR2 phosphorylation in response to heparin (10 μg/ml) than did the $Ndst1^{+/+}Ndst2^{+/+}$ and $Ndst1^{+/+}Ndst2^{-/-}$ cells ($P < 0.05$, *t*-test). Heparin alone had no effect on Erk or VEGFR2 phosphorylation (data not shown).

HEPARIN MODULATION OF VEGF-VEGFR2 RECEPTOR BINDING

Because both VEGF-A_{165} and VEGFR2 bind heparin [Gitay-Goren et al., 1992; Dougher et al., 1997], an additional mechanism for heparin enhancement of VEGF activity is the cross-bridging or stabilization of the VEGF-VEGFR2 complex by heparin. Surface plasmon resonance (SPR) techniques were used to measure VEGF-A binding to VEGFR2 in a cell-free system in real-time. Unfractionated heparin promoted VEGF-A binding to VEGFR2, with maximal binding observed at 1 μg/ml heparin (Fig. 3A). At higher concentrations of heparin (100 μg/ml), binding was inhibited. Low molecular weight heparins (≤5,000 Da) did not enhance VEGF-A binding (Fig. 3B).

STRUCTURAL SPECIFICITY OF HEPARIN-VEGF BINDING BY SPR

To investigate the structural specificity of heparin binding to VEGF-A, we immobilized a library of heparin and other sulfated glycosaminoglycan partial structures onto "array type sugar

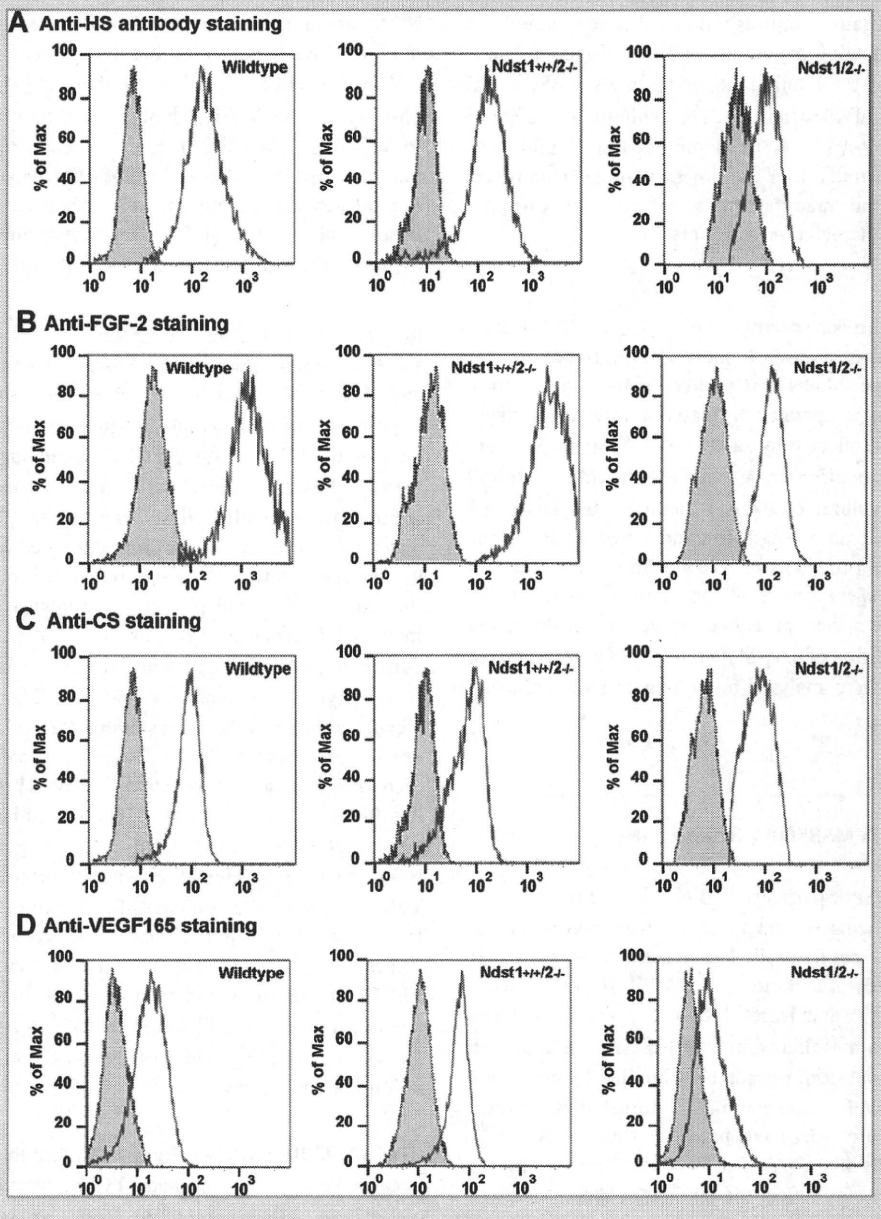

Fig. 1. Analysis of cell surface glycosaminoglycan sulfation in mouse endothelial cells lacking the Ndst enzymes. Flow cytometry was employed to phenotype the surface expression of sulfated heparans in mouse endothelial cells of these genotypes: Ndst1$^{+/+}$Ndst2$^{+/+}$ (wild-type), Ndst1$^{+/+}$Ndst2$^{-/-}$ and Ndst1$^{-/-}$Ndst2$^{-/-}$. Cells were exposed to the primary antibody or biotinylated ligand, and then stained with a secondary FITC-conjugated goat anti-mouse IgM or with FITC-streptavidin. In each panel, the gray histograms represent controls (either irrelevant primary isotype antibody, or only the secondary antibody), and the red histograms are cells stained with the antibody of interest. Panel A: Anti-heparan sulfates antibody that is sulfation specific; (B) biotinylated FGF-2; (C) anti-chondroitin sulfates (anti-CS) antibody; (D) biotinylated VEGF-A_{165}. Data are representative of three separate experiments.

chips" and measured their kinetic binding of VEGF-165. Table I summarizes these findings. Among the heparin partial structures, those containing glucosamine *N*-sulfates 6-*O*-sulfates (GlcNS6S) had lower K_D, independent of the presence or absence of 2-*O*-sulfation at the iduronic/glucuronic acid residue. For the chondroitin sulfates partial structures, 6-*O*-sulfation of the *N*-acetylgalactosamine (GalNAc) moiety conferred a lower K_D than did 4-*O*-sulfation.

HEPARIN MODULATION OF VEGF SECONDARY STRUCTURE

Circular dichroism spectra were measured from VEGF-A_{165} alone, and after the sequential addition of increments of unfractionated heparin. Control spectra were obtained from heparin alone, as well as heparin with VEGF-A_{121}, which does not bind heparin. Sequential additions of heparin reached a maximal effect at 0.5 μM heparin, and no additional conformational change was observed at higher concentrations. Figure 4 shows that the negative peak of VEGF-A_{165}

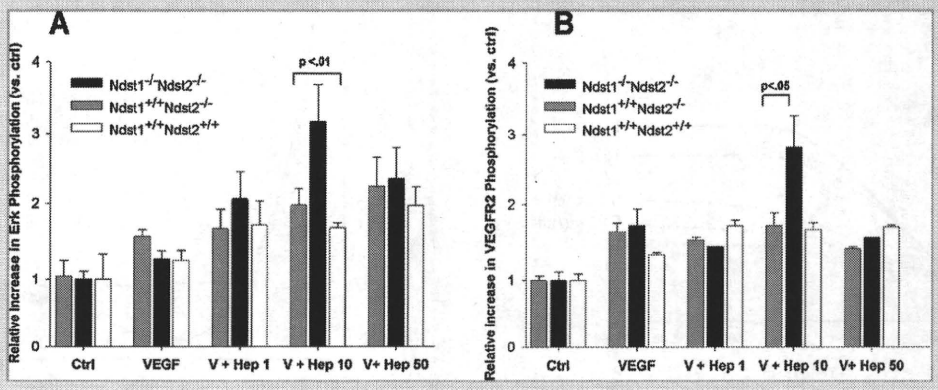

Fig. 2. VEGF-mediated Erk and VEGFR2 phosphorylation in mouse endothelial cells lacking heparan sulfates. Mouse endothelial cell-lines lacking heparan sulfates ($Ndst1^{-/-}Ndst2^{-/-}$) and normally sulfated mouse endothelial cell-lines ($Ndst1^{+/+}Ndst2^{+/+}$ and $Ndst1^{+/+}Ndst2^{-/-}$) were incubated in serum-free MCDB 131 medium for 2 h prior to stimulation with VEGF-A for 5 min. Control cultures (Ctrl) received no VEGF-A or heparin treatment. Remaining cultures were stimulated with VEGF-A (5 ng/ml) with or without heparin at the indicated concentrations. V + Hep 1, V + Hep 10 and V + Hep 50 denotes VEGF-A (5 ng/ml), plus heparin 1 μg/ml, 10 μg/ml and 50 μg/ml respectively. A: Phosphorylated Erk and (B) VEGFR2 levels were measured by Western blotting and quantified as described in the Materials and Methods Section. Values are means ± SEM (n = 3). Statistical significance was determined by the Wilcoxon rank-sum test. In each panel, the $Ndst1^{-/-}Ndst2^{-/-}$ was significantly higher than its indicated comparators.

shifted from a minimum at 200.6–209.0 nm. Addition of heparin to VEGF-A_{121} showed no change; the spectra were virtually identical in the absence of heparin and at all concentrations of added heparin (data not shown). The CD spectra of VEGF-A_{165} were also measured in response to a low molecular weight (~5,000) and high molecular weight heparin (~21,000), and the relative changes in secondary structure were compared to the standard unfractionated heparin (~15,000) using an average of the algorithms of Chen, Bolotina, and Chang (Table II). Spectral shifts were essentially complete at a molar ratio of heparin/VEGF-A of 0.54 for the low molecular weight heparin, and 0.36 for the unfractionated and high molecular weight heparins. The secondary structure of VEGF-A alone was predominantly random coil and β-sheet, with lesser elements of β-turn and α-helix respectively. Table II shows that upon the addition of saturating concentrations of heparins, the proportion of α-helix increased significantly in proportion to the molecular weight of the heparin.

DISCUSSION

The biosynthesis of heparan sulfate is a complex process, involving more than 26 enzymes. In particular, Ndst catalyzes the deacetylation and *N*-sulfation of the *N*-acetylglucosamine residues in heparan sulfates and plays an essential role in generation of ligand binding sites in mature heparan sulfates. Four related *Ndst* genes are identified (*Ndst1-4*). However in mouse lung endothelial cells only Ndst1 and Ndst2 are abundantly expressed. In our previous studies, we derived $Ndst2^{-/-}$ and its daughter $Ndst1^{-/-}Ndst2^{-/-}$ mouse lung endothelial cells [Wang et al., 2005]. In this current study, we employed these endothelial cell lines to further define how heparins modulate VEGF-A biological effects. Cells lacking the Ndst2 enzyme ($Ndst1^{+/+}Ndst2^{-/-}$) still express normal levels of sulfated heparans, and in these experiments they showed a typical response to heparin: enhancement of VEGF-A effects at low concentrations. However, in cells lacking both Ndst enzymes ($Ndst1^{-/-}Ndst2^{-/-}$) which are devoid of sulfated heparans, exogenous heparin dramatically enhanced VEGF response to VEGFR2 and Erk phosphorylation. One hypothesis is that under normal conditions, heparan sulfate proteoglycans (HSPGs) modulate VEGF-A biological responses in both directions – that is, enhance VEGF signaling but also moderate it. On the positive side, the cell-surface HSPGs are binding sites for VEGF-A, enhancing and stabilizing its binding to its cognate tyrosine receptor kinases. In the absence of sulfated heparans, VEGF–cell interactions would be less effective (as observed especially for VEGFR2, the immediate cellular responder), and exogenous heparin would enhance VEGF-cell binding through cross-bridging effects. On the inhibitory side, engagement of VEGF-A with HSPGs could produce counter-regulatory effects, independently modulating the conventional pathways to VEGF-A activation of the cell. Thus, cells lacking sulfated HSPGs would show even greater enhancement of VEGF-A by exogenous heparin, because they lack the intrinsic counter-regulation initiated by independent HSPG signaling. We recognize that this is a speculative theory, which will require more extensive, focused experiments to confirm or deny it. However, one abundant family of HSPGs, the syndecans, are known to signal independently through their cytoplasmic domains [Oh et al., 1997], and other studies have shown that HSPG can inhibit transforming growth factor beta and platelet derived growth factor signaling [Koyama et al., 1998; Chen et al., 2006].

This research also examined cell-independent mechanisms for heparin's effects. We found in cell-free systems that heparin enhanced the binding of VEGF-A to VEGFR2. However, the concentration of heparin (1 μg/ml) required for maximal VEGF-A binding to VEGFR2 was 10-fold less when compared to the concentration of heparin (10 μg/ml) required for optimal VEGF-A induced Erk activation and VEGFR2 phosphorylation. One plausible explanation for the discrepancy in the optimal concentrations of heparin required in the two assays is that the binding assays were

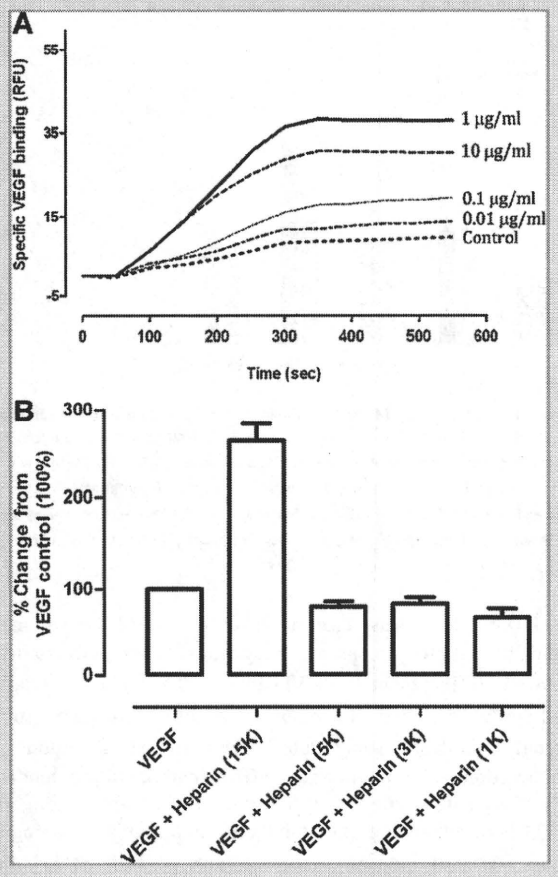

Fig. 3. Heparin modulation of VEGF-A binding to VEGFR2. SPR technology was employed to measure VEGF-A binding to immobilized VEGFR2, as described in the Materials and Methods Section. A: Various concentrations of unfractionated heparin (average molecular weight ~15 kDa) mixed with VEGF-A (5 ng/ml) were injected over immobilized VEGFR2-Fc chimera at a flow rate of 15 μl/min. B: Different molecular weight heparins (1 μg/ml) mixed with VEGF-A (5 ng/ml) were injected over immobilized chimeric VEGFR2-Fc protein at a flow rate of 15 μl/min. Data are presented as means ± SEM (n = 3).

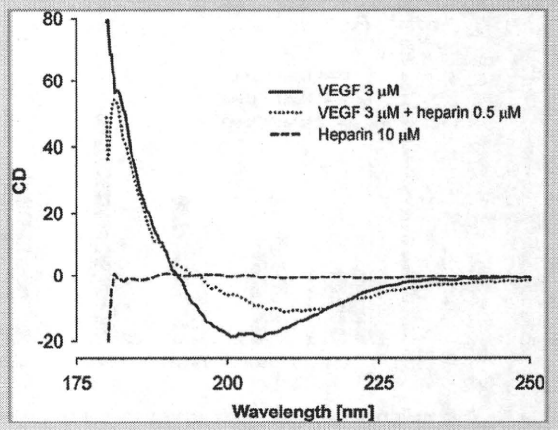

Fig. 4. Circular dichroism spectra of VEGF-A_{165}. Spectral scans were obtained as described in the Materials and Methods Section. Upon the addition of increments of heparin, there was a maximal shift in the negative peak of VEGF from 200.6 to 209 nm, at a heparin concentration of 0.5 μM. Heparin alone showed no shift in the area of interest.

carried out in a cell-free system so that heparin can bind to only VEGF or VEGFR2. However, the Erk and VEGFR2 phosphorylation assays were carried out in endothelial cell lines. In this system, heparin can bind not only to VEGF-A and VEGFR2 but to other ligands that are on the endothelial cell surface and thus a higher concentration of heparin was needed for promoting optimal VEGF-A responses.

Considering that both the VEGF-A and VEGFR2 bind heparin [Dougher et al., 1997], these data suggest that exogenous heparin may also play a cross-bridging role in supporting and sustaining the engagement of the protein ligand with its receptor. This behavior mirrors the effects of heparin on another growth factor/receptor complex, FGF, in which heparin forms a ternary complex with the ligand and receptor [Pellegrini et al., 2000]. In both cases, receptor dimerization contributes to signaling [Li et al., 2008], although unlike FGF, VEGF already exists as a natural dimer. Thus, the current binding studies strongly suggest that the biophysical actions of heparins in FGF-receptor interactions may also apply to VEGF-receptor interactions.

TABLE I. Structural Specificity of VEGF Binding to Defined Glycosaminoglycan Structures

Sugar sequence	Partial structure of	K_D (nM)	$k_a \times 10^3$ (M^{-1} sec^{-1})	$k_d \times 10^{-3}$ (sec^{-1})
GlcAβ1-3GalNAc4Sβ1-6Glc	Chondroitin sulfates A	34.1	115.6	3.94
GlcAβ1-3GalNAc6Sβ1-6Glc	Chondroitin sulfates C	14.7	111.0	1.64
GlcA2Sβ1-3GalNAc6Sβ1-6Glc	Chondroitin sulfates D	12.6	88.7	1.12
GlcAβ1-3GalNAc4S6Sβ1-6Glc	Chondroitin sulfates E	19.6	64.6	1.26
GlcNSα1-4GlcAβ1-6Glc	Heparin	66.1	62.7	4.15
GlcNSα1-4IdoA2Sα1-6Glc	Heparin	46.8	68.4	3.20
GlcNS6Sα1-4GlcAβ1-6Glc	Heparin	12.0	88.0	1.05
GlcNS6Sα1-4IdoA2Sα1-6Glc	Heparin	16.5	78.5	1.30
GlcAβ1-6Glc	Control	151.9	73.9	11.23
Galβ1-4Glc	Control	NB	NB	NB
Glcβ1-6Glc	Control	NB	NB	NB
Unfractionated heparin	Heparin	11.3	49.1	0.56

Surface Plasmon Resonance studies were performed as described in the Materials and Methods Section, using a multi-channel analyzer and a sugar-chip array immobilized with the defined synthetic structures indicated. Dissociation constant (K_D), on-rate (k_a), and off-rate (k_d) were calculated from multiple runs, using the manufacturer's software. NB, no binding.

TABLE II. Changes in the Estimated Percentages of Secondary Structure of VEGF in Response to Heparins

	α-Helix	β-Sheet	β-Turn	Random coil	Total
VEGF alone	5	32	20	43	100
LMWH	9	25	22	44	100
Unfx heparin	15	22	22	41	100
HMWH	33	1	24	42	100

CD spectra were obtained in the absence and presence of saturating concentrations of heparin (0.9 mol/mol LMWH/VEGF, 0.35 mol/mol for unfractionated (unfx) and high molecular weight heparin (HMWH). The percentage of secondary structure was estimated using the average of 3 algorithms, calculated from two independent spectral scans each.

An additional, cell-independent effect of heparin was documented by circular dichroism studies. Heparin binding to VEGF-A_{165} induced a shift in the protein's negative peak from 200.6 to 209 nm. No change was seen with heparin alone, or when heparin was added to VEGF-A_{121}. This heparin-induced spectral shift in VEGF-165 corresponded to an increase in the helix content of the protein which was proportional to the molecular weight of the heparin. Heparin is known to modulate the secondary structure of a number of heparin-binding proteins, including the classic case of antithrombin III [Stone et al., 1982; Tyler-Cross et al., 1996] and FGF [Prestrelski et al., 1992]. In previous work with antithrombin III, we have shown that heparin specifically increases the helical content of that protein [Ferran et al., 1992]. There are also precedents from other proteins to suggest that shifts in helix content induced by heparin may affect the biological function of the protein [Almeida et al., 1999]. However, further functional studies will be needed to confirm this for VEGF. We have used the terms heparin and heparan both of which share the same core disaccharide structure, but differ in the density and distribution of sulfated regions. Heparans are less sulfated overall, but in their areas of higher sulfation they resemble heparin in its type and density of sulfation [Robinson et al., 2006].

The effects of a 2-*O*-sulfation in the uronic acid moiety (glucuronic or iduronic) on VEGF-A binding are very modest, if noticeable at all. For an *N*- and 6-*O*-sulfated structure, the presence or absence of a 2-*O* sulfate makes very little difference K_D (12 vs. 16.5). Likewise, starting with a single *N*-sulfated structure, the addition of a 2-*O* sulfate has only a modest effect on the K_D (66 vs. 47), compared with the dramatic effect of adding a 6-*O* sulfate (66 vs. 12). A similar tendency was shown in the case of the partial structures of chondroitin sulfates. The 2-*O*-sulfation of the glucuronic acid did not affect the K_D (13 vs. 15 or 20), but the 6-*O*-sulfation more dramatically affected the K_D (34 vs. 15). This suggests that the interaction depends on the 6-*O*-sulfated structure more than that of the net charge, or the 2-*O* sulfation. These findings are indeed in keeping with the research of Robinson et al. [2006] and Ono et al. [1999]. Looking across different glycosaminoglycan families there are similarities and differences between the structural determinants. For dermatan and heparan, 6-*O* sulfation of the hexosamine residue appears to be important for binding HGF and VEGF, while 2-*O* sulfation of iduronic residues is not essential [Lyon et al., 1994, 1998]. Lyon et al. has found that for dermatan sulfates, the iduronic residue appears to be quite important, yet not so critical for heparins/heparans. Holmborn et al. [2004] observed that heparan sulfate synthesized by the Ndst1 and Ndst2 double mutant mouse embryonic stem cells is still 6-*O*-sulfated but contains no *N*- and 2-*O*-sulfate groups. Our recent studies observed both Ndst1 and Ndst2 are abundantly expressed in endothelial cells [Wang et al., 2005]. Chemical analysis of heparan sulfate synthesized by the Ndst1 and Ndst2 double mutant endothelial cells showed a similar heparan sulfate structural change as reported for the Ndst1 and Ndst2 double mutant mouse embryonic stem cells. The endothelial heparan sulfate structure alteration caused by the Ndst1 and Ndst2 ablation inhibited FGF-2 and VEGF-A binding, which are known to depend on *N*- and/or 2-*O*-sulfation.

We believe that the sulfation pattern of the glycosaminoglycan may be only one of the important determinants for modulation of the complex processes of VEGF-mediated cellular responses. In fact polymer size, as well as the configuration of sulfated domains may be as important for the pro-angiogenic activities of a heparin as are the unique disaccharide structure and specific sulfation. Robinson et al. [2006] has suggested that a heparan sulfate polysaccharide containing a pair of highly sulfated heparin-like regions separated by an unsulfated region functions as a binary ligand that can form a more stable VEGF-heparin complex. Throughout our studies, heparins of larger polymer chain length were more effective in inducing Erk phosphorylation, in promoting VEGF-VEGFR2 binding, and in inducing a conformational change in the VEGF protein. The molecular weight dependency of these processes was also borne out by the work of Rouet et al. [2005], who developed a high molecular weight heparin-mimetic polymer that further promoted VEGF activity. Studies by Mamluk et al. [2002] show that heparin can bind neurophilin and increase the affinity of that heparin–VEGF interaction. Therefore polymer size as well as the site-specificity of sulfations may play a role in promoting the binding of VEGF with both VEGFR2 and neurophilin to form a ternary complex with strong signaling capability.

In conclusion, these data show that exogenous heparin enhances VEGF-induced cellular responses much more significantly in cells lacking sulfated HSPGs, compared with cells that are sulfated. A plausible explanation is that while both cell types benefit from the pro-angiogenic stimuli of preformed VEGF-heparin complexes, the unsulfated cells may be free of the negative feedback induced by growth factor binding to signaling HSPGs like syndecans. Heparin appears to play important biophysical roles for VEGF-A. Heparin promotes VEGF-A binding to its receptor, and likely forms a ternary VEGF-heparin-VEGFR2 complex. Heparin also alters the conformation of VEGF-A_{165} protein. The specificity of heparin's actions lies in part in the pattern of sulfation sites, but also appears to depend on the polymer chain length, as one would expect for a cross-bridging role. Our knowledge of VEGF–heparin interactions is still not as far advanced as it is for the FGF system or other growth factors. We are hopeful that this current work will be helpful in refining glycosaminoglycans that can ultimately be employed as modulators of angiogenesis.

ACKNOWLEDGMENTS

This research was supported by grants from NIH (RO1HL097182 to M.S. and P41RR005351 to L.W. with James H. Prestegard as the PI) and the Japan Science and Technology Agency to Y.S.

REFERENCES

Almeida PC, Nantes IL, Rizzi CC, Judice WA, Chagas JR, Juliano L, Nader HB, Tersariol IL. 1999. Cysteine proteinase activity regulation. A possible role of heparin and heparin-like glycosaminoglycans. J Biol Chem 274:30433–30438.

Ashikari-Hada S, Habuchi H, Kariya Y, Kimata K. 2005. Heparin regulates vascular endothelial growth factor165-dependent mitogenic activity, tube formation, and its receptor phosphorylation of human endothelial cells. Comparison of the effects of heparin and modified heparins. J Biol Chem 280:31508–31515.

Carmeliet P, Ferreira V, Breier G, Pollefeyt S, Kieckens L, Gertsenstein M, Fahrig M, Vandenhoeck A, Harpal K, Eberhardt C, Declercq C, Pawling J, Moons L, Collen D, Risau W, Nagy A. 1996. Abnormal blood vessel development and lethality in embryos lacking a single VEGF allele. Nature 380:435–439.

Chen CL, Huang SS, Huang JS. 2006. Cellular heparan sulfate negatively modulates transforming growth factor-beta1 (TGF-beta1) responsiveness in epithelial cells. J Biol Chem 281:11506–11514.

Dougher AM, Wasserstrom H, Torley L, Shridaran L, Westdock P, Hileman RE, Fromm JR, Anderberg R, Lyman S, Linhardt RJ, Kaplan J, Terman BI. 1997. Identification of a heparin binding peptide on the extracellular domain of the KDR VEGF receptor. Growth Factors 14:257–268.

Dvorak HF. 2005. Angiogenesis: Update 2005. J Thromb Haemost 3:1835–1842.

Ferran DS, Sobel M, Harris RB. 1992. Design and synthesis of a helix heparin-binding peptide. Biochemistry 31:5010–5016.

Ferrara N, Gerber HP, LeCouter J. 2003. The biology of VEGF and its receptors. Nat Med 9:669–676.

Gitay-Goren H, Soker S, Vlodavsky I, Neufeld G. 1992. The binding of vascular endothelial growth factor to its receptors is dependent on cell surface-associated heparin-like molecules. J Biol Chem 267:6093–6098.

Holmborn K, Ledin J, Smeds E, Eriksson I, Kusche-Gullberg M, Kjellen L. 2004. Heparan sulfate synthesized by mouse embryonic stem cells deficient in NDST1 and NDST2 is 6-*O*-sulfated but contains no *N*-sulfate groups. J Biol Chem 279:42355–42358.

Koyama N, Kinsella MG, Wight TN, Hedin U, Clowes AW. 1998. Heparan sulfate proteoglycans mediate a potent inhibitory signal for migration of vascular smooth muscle cells. Circ Res 83:305–313.

Lake AC, Vassy R, Di BM, Lavigne D, Le VC, Perret GY, Letourneur D. 2006. Low molecular weight fucoidan increases VEGF165-induced endothelial cell migration by enhancing VEGF165 binding to VEGFR-2 and NRP1. J Biol Chem 281:37844–37852.

Li X, Claesson-Welsh L, Shibuya M. 2008. VEGF receptor signal transduction. Methods Enzymol 443:261–284.

Lyon M, Deakin JA, Mizuno K, Nakamura T, Gallagher JT. 1994. Interaction of hepatocyte growth factor with heparan sulfate. Elucidation of the major heparan sulfate structural determinants. J Biol Chem 269:11216–11223.

Lyon M, Deakin JA, Rahmoune H, Fernig DG, Nakamura T, Gallagher JT. 1998. Hepatocyte growth factor/scatter factor binds with high affinity to dermatan sulfate. J Biol Chem 273:271–278.

Mamluk R, Gechtman Z, Kutcher ME, Gasiunas N, Gallagher J, Klagsbrun M. 2002. Neuropilin-1 binds vascular endothelial growth factor 165, placenta growth factor-2, and heparin via its b1b2 domain. J Biol Chem 277:24818–24825.

Neufeld G, Cohen T, Gengrinovitch S, Poltorak Z. 1999. Vascular endothelial growth factor (VEGF) and its receptors. FASEB J 13:9–22.

Oh ES, Woods A, Couchman JR. 1997. Syndecan-4 proteoglycan regulates the distribution and activity of protein kinase C. J Biol Chem 272:8133–8136.

Ono K, Hattori H, Takeshita S, Kurita A, Ishihara M. 1999. Structural features in heparin that interact with VEGF 165 and modulates its biological activity. Glycobiology 9:705–711.

Park M, Lee ST. 1999. The fourth immunoglobulin-like loop in the extracellular domain of FLT-1, a VEGF receptor, includes a major heparin-binding site. Biochem Biophys Res Commun 264:730–734.

Pellegrini L, Burke DF, von DF MulloyB, Blundell TL. 2000. Crystal structure of fibroblast growth factor receptor ectodomain bound to ligand and heparin. Nature 407:1029–1034.

Poletti LF, Bird KE, Marques D, Harris RB, Suda Y, Sobel M. 1997. Structural aspects of heparin responsible for interactions with von Willebrand factor. Arterioscler Thromb Vasc Biol 17:925–931.

Prestrelski SJ, Fox GM, Arakawa T. 1992. Binding of heparin to basic fibroblast growth factor induces a conformational change. Arch Biochem Biophys 293:314–319.

Robinson CJ, Mulloy B, Gallagher JT, Stringer SE. 2006. VEGF165-binding sites within heparan sulfate encompass two highly sulfated domains and can be liberated by K5 lyase. J Biol Chem 281:1731–1740.

Rouet V, Hamma-Kourbali Y, Petit E, Panagopoulou P, Katsoris P, Barritault D, Caruelle JP, Courty J. 2005. A synthetic glycosaminoglycan mimetic binds vascular endothelial growth factor and modulates angiogenesis. J Biol Chem 280:32792–32800.

Soker S, Takashima S, Miao HQ, Neufeld G, Klagsbrun M. 1998. Neuropilin-1 is expressed by endothelial and tumor cells as an isoform-specific receptor for vascular endothelial growth factor. Cell 92:735–745.

Stone AL, Beeler D, Oosta G, Rosenberg RD. 1982. Circular dichroism spectroscopy of heparin-antithrombin interactions. Proc Natl Acad Sci USA 79:7190–7194.

Suda Y, Marques D, Kermode JC, Kusumoto S, Sobel M. 1993. Structural characterization of heparins binding domain for human platelets. Thromb Res 69:501–508.

Suda Y, Arano A, Fukui Y, Koshida S, Wakao M, Nishimura T, Kusumoto S, Sobel M. 2006. Immobilization and clustering of structurally defined oligosaccharides for sugar chips: An improved method for surface plasmon resonance analysis of protein-carbohydrate interactions. Bioconjug Chem 17:1125–1135.

Tischer E, Mitchell R, Hartman T, Silva M, Gospodarowicz D, Fiddes JC, Abraham JA. 1991. The human gene for vascular endothelial growth factor. Multiple protein forms are encoded through alternative exon splicing. J Biol Chem 266:11947–11954.

Tyler-Cross R, Sobel M, McAdory LE, Harris RB. 1996. Structure-function relations of antithrombin III-heparin interactions as assessed by biophysical and biological assays and molecular modelling of peptide pentasaccharide docked complexes. Arch Biochem Biophys 334:206–213.

Wakao M, Saito A, Ohishi K, Kishimoto Y, Nishimura T, Sobel M, Suda Y. 2008. Sugar chips immobilized with synthetic sulfated disaccharides of heparin/heparan sulfate partial structure. Bioorg Med Chem Lett 18:2499–2504.

Wang L, Fuster M, Sriramarao P, Esko JD. 2005. Endothelial heparan sulfate deficiency impairs L-selectin- and chemokine-mediated neutrophil trafficking during inflammatory responses. Nat Immunol 6:902–910.

Wijelath ES, Rahman S, Namekata M, Murray J, Nishimura T, Mostafavi-Pour Z, Patel Y, Suda Y, Humphries MJ, Sobel M. 2006. Heparin-II domain of fibronectin is a vascular endothelial growth factor-binding domain: Enhancement of VEGF biological activity by a singular growth factor/matrix protein synergism. Circ Res 99:853–860.

Carboxymethyl-chitin promotes chondrogenesis by inducing the production of growth factors from immune cells

Hiroyuki Kariya,[1] Yusuke Yoshihara,[2] Yumiko Nakao,[2] Nobuko Sakurai,[2] Masaru Ueno,[2] Masahito Hashimoto,[1] Yasuo Suda[1]

[1]Department of Nanostructure and Advanced Materials, Graduate School of Science and Engineering, Kagoshima University, Kagoshima, Japan
[2]Japan Medical Materials Corporation, Osaka, Japan

Received 7 October 2008; revised 28 November 2009; accepted 14 December 2009
Published online 31 March 2010 in Wiley InterScience (www.interscience.wiley.com). DOI: 10.1002/jbm.a.32771

Abstract: Many techniques have been tested for their ability to restore cartilage defects, but several problems still remain in the complete healing of injured cartilage. In our previous study, we found that a carboxymethyl-chitin/β-tricalcium phosphate (CM-chitin/β-TCP) composite induced cartilage regeneration in the osteochondral defects of rabbits *in vivo*. We also found that CM-chitin stimulated peritoneal exudate cells (PEC) in mice and induced several kinds of inflammatory cytokines and transforming growth factor beta-1 (TGF-β1). In this study, we examined whether CM-chitin is responsible for the induction of chondrogenesis via the production of TGF-β1 *in vitro*. The murine pluripotent cell line C3H10T1/2 was maintained as a micromass culture in conditioned medium prepared from PEC stimulated with and without CM-chitin. CM-chitin–conditioned medium induced RNA expression of the chondrogenic-factor Sox9 and the matrix proteins aggrecan, Col2a1, and Comp. Their expression levels were decreased in the presence of anti-TGF-β1 antibody. The micromass tissues cultured in CM-chitin conditioned medium at day 21 were clearly stained by Toluidine blue or Alcian blue (histological staining) and collagen II antibody (immunohistological staining), showing the expression of acidic glycosaminoglycan and type II collagen. Similar results were observed in micromass tissue stimulated with TGF-β1 as a positive control. However, no chondrogenesis occurred when CM-chitin was added directly to a C3H10T1/2 cell culture. These results indicated that CM-chitin is a potent inducer of chondrogenesis via the induction of TGF-β1 in immune cells. © 2010 Wiley Periodicals, Inc. J Biomed Mater Res Part A: 94A: 1034–1041, 2010.

Key Words: CM-chitin, chondrogenesis, TGF-β, micromass culture, PEC

INTRODUCTION

Cartilage is known to have a poor capacity for self-repair because of its low mitotic activity and avascular nature.[1,2] Several medical and surgical methods have been tested for their ability to repair cartilage defects, but complete regeneration of normal cartilage in damaged areas is difficult to achieve due to several problems such as the loosening of artificial joints, degenerative changes in transplanted tissues,[3] and the risk of viral transmission.[4,5]

Recently, tissue-engineering approaches using biocompatible scaffolds have been applied to the treatment of cartilage defects,[4,6–9] and many materials such as collagen,[10] hydroxyapatite,[11,12] polyglycolic acid,[13] hyaluronic acid,[14,15] and silk[6,7] have been investigated. Such scaffolds play an important role in promoting the formation of cartilage as a temporary extracellular matrix (ECM). In many cases, the scaffold-based tissue-engineering technique requires the addition of growth factors, such as transforming growth factor-beta (TGF-β) or bone morphogenetic protein (BMP). It is well known that these growth factors promote the proliferation or differentiation of chondrocytes from mesenchymal stem cells *in vivo*[16–19] and *in vitro*.[4,7,20,21] Although tissue-engineering techniques that combine scaffolds with growth factors have great potential for cartilage repair, they are still at an experimental stage because of the cost of using a large amount of expensive recombinant growth factors.

In our previous study, we found that a carboxymethyl-chitin (CM-chitin)/β-tricalcium phosphate (β-TCP) composite induced the regeneration of cartilage in the osteochondral defects of rabbits.[22] The regeneration of cartilage was observed after treatment with the CM-chitin/β-TCP composite but not with β-TCP alone 8 weeks after implantation, indicating that CM-chitin plays a key role in the regeneration of cartilage. Previously, we also showed that CM-chitin stimulated murine peritoneal exudate cells (PEC) to induce the expression of inflammatory cytokines and TGF-β1.[23] TGF-β1 has many functions,[24] including the induction of mesenchymal cell condensation, which is required for *in vitro* chondrogenesis.[25–27] However, no correlation between the stimulation of cells induced with CM-chitin and the regeneration of cartilage has been demonstrated.

The murine pluripotential cell line C3H10T1/2 has been shown to differentiate into myoblasts, osteoblasts, adipocytes, and chondrocytes after treatment with growth factors.[20] C3H10T1/2 cells are attractive for studying

Correspondence to: M. Hashimoto; e-mail: hassy@eng.kagoshima-u.ac.jp

chondrogenesis because they do not spontaneously differentiate under standard culture conditions. Previously, treatment of a high-density micromass culture of C3H10T1/2 cells with TGF-β1 was reported to induce the formation of a three-dimensional (3D) spheroid structure and chondrogenic differentiation.[20,28–30] In this study, we examined the effect of CM-chitin on chondrogenesis using the aforementioned *in vitro* micromass culture system.

MATERIALS AND METHODS

CM-chitin preparation and cell stimulation

The CM-chitin (degree of substitution for *O*-carboxymethylation = 79 mol %, degree of deacetylation = 27 mol %) was prepared from chitin extracted from Queen Crab shells, according to a previously reported method.[31] Gel-type CM-chitin was prepared as described[22] and suspended in phosphate-buffered saline (PBS) (10 mg/mL). The level of endotoxin contamination was determined by the Endospecy® test (Seikagaku Biobusiness, Tokyo, Japan) according to the manufacturer's instructions.

In this experiment, we used a PEC-utilizing micromass culture as an experimental model of chondrogenesis. Eight to ten-week-old male BALB/cN-sea mice were obtained from Kyudo (Saga, Japan). The animal experiment was performed in accordance with our institutional approval (H18Eng007) and guidelines and the legal requirements of Japan. The mice were injected intraperitoneally (ip) with 0.5 mL of PBS or CM-chitin gel suspension (1 mg/mL). After 24 h stimulation, the ip-administered mice were sacrificed, and 5 ml PBS were injected into the peritoneal cavity. After extracting peritoneal exudate fluid, we collected PEC from the fluid. The number of cells was $1–3 \times 10^6$ cells per mouse. After 24 h culture in Dulbecco's Modified Eagles Medium (DMEM) supplemented with 10% Fetal Bovine Serum (FBS, Equitech-Bio, Kerrville, Texas, USA), 100 unit/mL penicillin, and 100 μg/mL streptomycin, the supernatants were collected and subjected to ultra-filtration with Amicon Ultra-15 Centrifugal Filter Devices (Millipore, Billerica, MA). The supernatants were concentrated to a 1/45 volume and used as PBS conditioned medium (PBS-sup) and CM-chitin conditioned medium (CM-chitin-sup), respectively (Scheme 1).

Monolayer culture of C3H10T1/2 cells

The murine pluripotential cell line C3H10T1/2 (Health Science Research Resources Bank, Tokyo, Japan) was maintained as a monolayer culture in 25 or 75 cm^2 polystyrene tissue culture flasks (Becton Dickinson, Franklin Lakes, NJ) in DMEM supplemented with 10% FBS, 100 μg/mL penicillin, and 100 μg/mL streptomycin. The cells were incubated in a humidified incubator at 37°C and 5% CO_2, and the culture medium was changed every 3 days.

C3H10T1/2 cells were seeded on 24-well culture plates at 10^5 cells/well and cultured with PBS (10% in medium), CM-chitin solution (1 mg/mL), CM-chitin gel suspension (1 mg/mL), or recombinant TGF-β1 (10 ng/mL, PeproTecch, NJ) for 1–5 days. As a negative control, Triton X-100 was added to lyse the cells. The cell culture supernatants were collected every day and used in a cytotoxicity detection assay with a lactate dehydrogenase (LDH) assay kit (Roche Applied Science, Mannheim, Germany) in accordance with manufacturer's procedure. The viability of the remaining cells was determined by 0.5% Trypan blue staining of cells treated with trypsin before they were scraped off the wells. Data are expressed as the mean ± SE of three independent experiments. The LDH values and cell numbers of each group were analyzed for statistical significance using Welch's *t*-test. Total RNA was extracted from the cells at 7, 14, and 21 days, and the mRNA expression of growth factors and cartilage-related genes was analyzed using the reverse-transcriptase polymerase chain reaction (RT-PCR) as described previously.[23] The pairs of primer sequences used were as follows: For β-actin: 5′-ATGGATGACGATATCGCT-3′ (sense) and 5′-ATGAGGTAGTCTGTCAGGT-3′ (antisense). For TGF-β1: 5′-TACTATGCTAAAGAGGTCACCC-3′ (sense) and 5′-TCCTTGGTTCAGCCACTGCC-3′ (antisense). For Agr: 5′-AGTG GATCGGTCTGAATGACAGG-3′ (sense) and 5′-AGAAGTTGT CAGGCTGGTTTGGA-3′ (antisense). For Col2a1: 5′-AGGGCAA CAGCAGGTTCACATAC-3′ (sense) and 5′-TGTCCACACCAAATT CCTGTTCA-3′ (antisense).

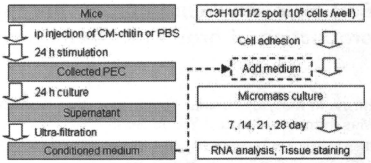

SCHEME 1. A procedure for micromass culture. The conditioned media were prepared separately and applied to micromass culture.

Micromass culture

The micromass culture experiment was performed according to the protocol of Ahrens et al.[32] with slight modifications (Scheme 1). In brief, the C3H10T1/2 cells were trypsinized and resuspended in DMEM medium containing 10% FBS (basic medium) at a concentration of 2×10^7 cells/mL, and 10 μL of the suspension were transferred to a 48-well culture plate and allowed to adhere for 1 h at 37°C in 5% CO_2. After the addition of 80 μL of basic medium and 20 μL of PBS, recombinant TGF-β1 (10 ng/mL), or one of the conditioned media (PBS-sup or CM-chitin-sup), the cells were cultured at 37°C in 5% CO_2. The medium was changed every 4 days, and micromass tissues were collected at 7, 14, 21, and 28 days. For the TGF-β1 blocking experiment, anti-TGF-β1 mAb (R&D systems, Tokyo, Japan) were added in TGF-β1 medium or CM-chitin-sup at 10 μg/mL and incubated for 1 h at room temperature before being used for the micromass culture. Each collected micromass tissue was used for mRNA expression analysis or histological staining.

RNA extraction, cDNA synthesis, and PCR analysis

The total cellular RNA was extracted from the micromass tissue. RT-PCR was performed using the SideStepTM II QPCR cDNA Synthesis Kit (Stratagene, CA), and consecutive

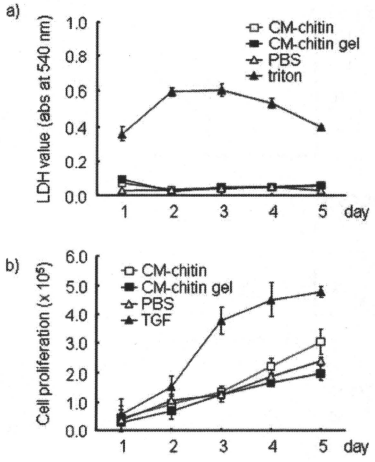

FIGURE 1. Cytotoxic and proliferative assay for CM-chitin. (a) Cytotoxicity was evaluated with a lactate dehydrogenase (LDH) assay. Each LDH value represented the cytotoxicity of the respective reagent. The cells in the triton group were disrupted by triton reagent, so the LDH-data of this group was used as a negative control. (b) Cell proliferation was determined by cell counting using a hemocytometer from days 1 to 5.

quantitative polymerase chain reactions (Q-PCR) were performed using SYBR Premix Ex Taq (Takara Bio, Shiga, Japan), according to the manufacturer's procedure. The sense and antisense primers for glyceraldehyde-3-phosphate dehydrogenase (GAPDH), aggrecan (Agr), collagen-2a1 (Col2a1), cartilage oligomeric matrix protein (Comp), sex-determining region Y-box9 (Sox9), collagen-1a1 (Col1a1), and collagen-10a1 (Col10a1) were purchased from Takara Bio (Shiga, Japan). The amplified products were analyzed using the 7300 Real-Time PCR System (Applied Biosystems, CA), and the transcription level normalized to GAPDH was then calculated using the 2^{Δ} *Ct* formula with reference to the undifferentiated mesenchymal stem cells.

Histology and immunohistology

After 21 and 28 days, the collected micromass tissues were rinsed with PBS, fixed with 4% formaldehyde for 30 min, and washed twice with PBS. The tissues cultured in medium containing nothing, TGF-β1, PBS-sup, or CM-chitin-sup were collected on day 21 and stained with Alcian blue [pH 1.0, 1% Alcian blue 8 GX (Sigma-Aldrich, MO) in 0.1*M* HCl] overnight at 4°C and washed with PBS.

The tissues cultured in TGF-β1 or CM-chitin-sup until day 28 were embedded in paraffin, sectioned at 12 μm using a microtome, and deparaffinized. The tissues cultured in medium alone or with PBS-sup until day 28 were used directly for staining because they did not form 3D aggregates. One set of samples was stained by 0.05% Toluidine blue (pH7.0) before being washed with 99% EtOH. At the same time, the other set of samples was subjected to Protease K treatment and blocking treatment and incubated with Rabbit anti-mouse Collagen II polyclonal-antibody (ab21291, Abcam Japan, Tokyo, Japan) for 30 min. After being washed with Tris-buffered saline (TBS), the samples were incubated with the secondary antibody (EnVision™+ Rabbit/HRP, DAKO Japan, Kyoto, Japan) before being washed with TBS. The samples were then stained with a substrate (DAB+ Liquid, DAKO Japan) for 1 min and washed with water, before being observed with an IX70 microscope (Olympus Medical Systems, Tokyo, Japan).

RESULTS

Effect of CM-chitin on a monolayer culture of C3H10T1/2 cells

First, we checked the endotoxin level of CM-chitin using the Endospecy® test. As a result, only a small amount of endotoxin was detected in gel-type CM-chitin at 100 μg/mL.

We then investigated the effects of CM-chitin on cell viability, proliferation, and stimulation. The LDH values showed that neither CM-chitin nor CM-chitin gel affected the cell viability of C3H10T1/2 cells and that there was no significant difference between the two treatments [Fig. 1(a)]. The proliferation rates of the C3H10T1/2 cells treated with PBS, CM-chitin, and CM-chitin gel were similar during the culture period, while the proliferation rate of the cells treated with TGF-β1 was higher than those of the cells treated with other reagents, especially at 3–5 days of culturing [Fig. 1(b)]. The RNA expression of growth factors and two cartilage-related genes in the C3H10T1/2 cells in monolayer culture was not significantly different among the PBS, CM-chitin, CM-chitin gel, and TGF-β1–treated groups (Fig. 2).

Expression of chondrogenic markers in micromass culture

To examine whether CM-chitin-sup, a conditioned medium from PEC stimulated by CM-chitin gel, promotes chondro-

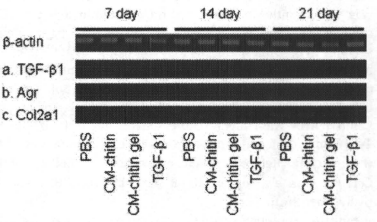

FIGURE 2. Effect of CM-chitin on monolayer culture of C3H10T1/2 cells. The cells were cultured as a monolayer in the presence of the indicated stimuli for 21 days. mRNA was obtained from the cells in each well and subjected to RT-PCR for the detection of TGF-β1, transforming growth factor-β1; Agr, aggrecan; and Col2a1, collagen2a1.

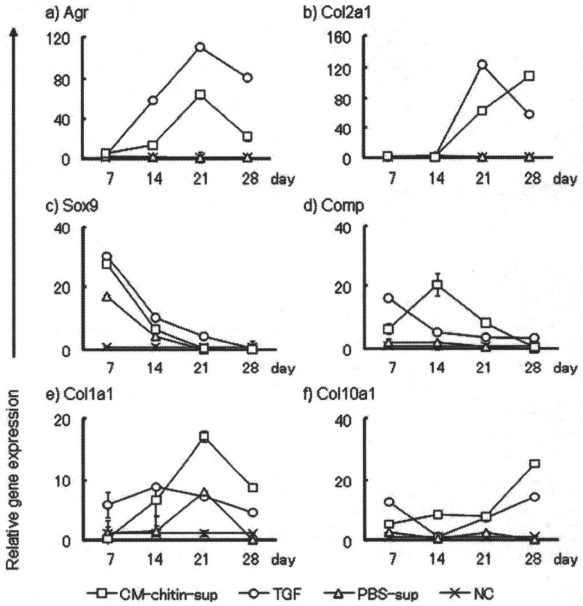

FIGURE 3. Quantitative mRNA expression of cartilage-related genes in micromass tissues. Micromass tissues were treated with TGF-β1 (10 ng/mL), PBS-conditioned medium (PBS-sup) or CM-chitin–conditioned medium (CM-chitin-sup) for 7, 14, 21, or 28 days, and their gene expression was compared with that of nontreated micromass tissue (NC). Data are expressed as the mean ± SE of three independent experiments. mRNA expression was normalized to that of GAPDH.

genesis in micromass culture, the mRNA expression of six chondrogenic markers in micromass tissues was quantified by Q-PCR. The mRNA expression of Agr and Col2a1 was significantly increased in the CM-chitin-sup treated samples on day 21, as well as in the TGF-β1–treated samples [Fig. 3(a,b)]. In the CM-chitin-sup treated micromass culture, the expression of Agr was found to be diminished on day 28, while the expression of Col2a1 was further increased on day 28 [Fig. 3(a,b)]. Sox9 and Comp mRNA were highly expressed on day 7 (Sox9) and 14 (Comp), but no expression was observed on day 28 [Fig. 3(c,d)]. Relatively high expression of Col1a1 and Col10a1 was also observed on days 21 and 28, respectively [Fig. 3(e)].

mRNA expression related to chondrogenesis was blocked by anti-TGF-β1 antibody (Fig. 4). The Agr, Co2a1, and Sox9 expression levels in the CM-chitin-sup and TGF-β1–treated micromass cultures were significantly decreased in the presence of the antibody.

Histological analysis of micromass culture

To examine whether the growth factors secreted from PEC stimulated by CM-chitin induce chondrogenesis, the accumulation of chondrogenesis-related ECM in the micromass tissues was investigated by staining with Alcian blue, Toluidine blue, and anti-Collagen II antibody. The specific aggregation of micromass tissues was observed in the TGF-β1–treated micromass culture and CM-chitin-sup treated micromass culture [Fig. 5(a)]. However, neither the non-treated micromass culture nor the PBS-sup treated micromass culture formed 3D aggregates.

In the presence of TGF-β1 or CM-chitin-sup, the tissues showed a strong blue color under Alcian blue staining [Fig. 5(a,b)] and a magenta color under Toluidine blue staining [Fig. 5(c)], indicating the presence of sulfated glycosaminoglycan.[33] Immunohistological staining also showed the presence of collagen II in these micromass tissues [Fig. 5(d)]. The micromass tissues collected on day 7 or 14 were also subjected to staining, but no marked staining was observed

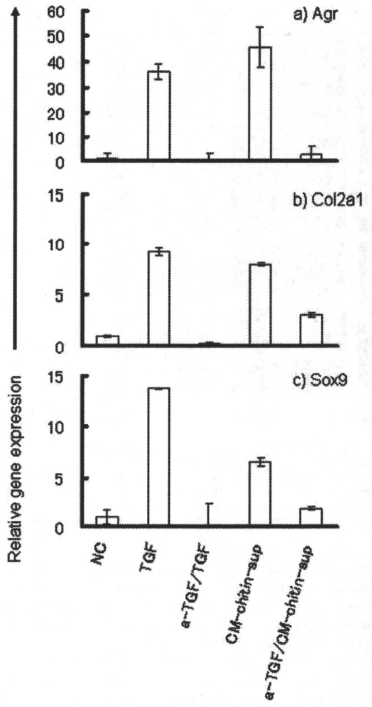

FIGURE 4. TGF-β1 blocking experiment using anti-TGF-β1 antibody. Micromass tissues were treated with TGF-β1 (TGF, 10 ng/mL), anti-TGF-β1 antibody + TGF-β1 (a-TGF/TGF, a-TGF = 10 μg/mL), CM-chitin-conditioned medium (CM-chitin-sup), or anti-TGF-β1 antibody + CM-chitin conditioned medium (a-TGF/CM-chitin-sup, a-TGF = 10 μg/mL), and their gene expression was compared with that of nontreated micromass tissues (NC). Micromass tissues were used for QPCR analysis of aggrecan (Agr), Collagen-2a1 (Col2a1), and Sox9 at the highest expression point of each gene (at days 21, 21, and 7, respectively). Data are expressed as the mean ± SE of three independent experiments. mRNA expression was normalized to that of GAPDH.

(data not shown). In contrast, the tissues treated with nothing or PBS-sup showed a weak blue color under Alcian blue staining and a blue color under Toluidine blue staining, indicating the absence of chondrogenesis-related ECM.

DISCUSSION

We previously reported that CM-chitin induced the regeneration of hyaline cartilage in rabbits *in vivo*.[22] In contrast to conventional scaffold-based tissue-engineering methods using growth factors, no growth factor is required in our CM-chitin–based method, suggesting that CM-chitin has dual functions, as a scaffold and an inducer of cartilage-differentiation. We, therefore, investigated whether CM-chitin directly affects the cartilage differentiation of progenitor cells. The murine pluripotent cell line C3H10T1/2 was used in the present study. CM-chitin did not significantly alter the viability or proliferation of the cells [Fig. 1(a,b)], similarly to other biomaterials, such as polylactic acid,[34] polylactic acid–polyglycolic acid,[35] poly(DL-lactic-*co*-glycolic acid),[36] and silk.[7,37] Furthermore, CM-chitin did not influence the expression of growth factor or chondrogenic markers in C3H10T1/2 cells (Fig. 2). These results indicate that CM-chitin did not contribute directly to the differentiation of pluripotent cells into chondrocytes.

We recently found that CM-chitin stimulates immune cells to produce TGF-β1, a growth factor for cartilage regeneration.[23] However, it was unclear whether the stimulation of cells by CM-chitin leads to cartilage regeneration. We demonstrated here that the factors secreted from cells stimulated by CM-chitin induced the expression of chondrogenic markers. Micromass tissue of C3H10T1/2 cells, cultured in the presence of CM-chitin-sup, expressed mRNA of chondrogenic markers including aggrecan and type II collagen (Fig. 3).

Agrrecan (Agr), type II collagen (Col2a1), and Sox9 are *in vivo* and *in vitro* markers of chondrogenesis. Agr is an integral part of ECM components in cartilage,[38–41] and its expression is induced by several factors including TGF-β1, TGF-β3, BMP-2, and dexamethasone in micromass culture, pellet culture, or an appropriate 3D culture.[42–46] TGF-β1 is reported to promote the expression of Col2a1 and Sox9.[47] Sox9, a transcription factor, acts during chondrocyte differentiation and activates the transcription of Agr and Col2a1.[40,48,49] Type II collagen, which includes an α-1 chain encoded by Col2a1, is the most abundant and important component of the chondrogenesis-related ECM, and mutations in this gene are associated with achondrogenesis and chondrodysplasia.[50,51] It has also been shown in previous studies that the expression of Col2a1 was accompanied by an increase in Agr or glycosaminoglycan expression during chondrogenesis.[52–54] The time-courses of the expression of Sox9, Col2a1, and Agr in the present study [Fig. 3(a–c)] were coincident with the results of the above reports. In our results, the expression of Agr was decreased in both the TGF-β1–treated micromass culture and CM-chitin–treated micromass culture at day 28 [Fig. 3(a)]; whereas, Col2a1 expression was increased in the CM-chitin–treated micromass culture while its expression was decreased in the TGF-β1–treated micromass culture at day 28 [Fig. 3(b)]. Previous research of murine limb-bud-cell micromass culture reported that the high expression of Col2a1 decreases gradually and that the expression of collagen10, which is commonly observed in hypertrophic cartilage, is replaced by Col2a1 expression.[27] In our experiment, the Col2a1 and Col10a1 expression in TGF-β1–treated micromass culture seemed to correspond with above mentioned report [Fig. 3(b,f)]. On the other hand, the Col2a1 and Col10a1

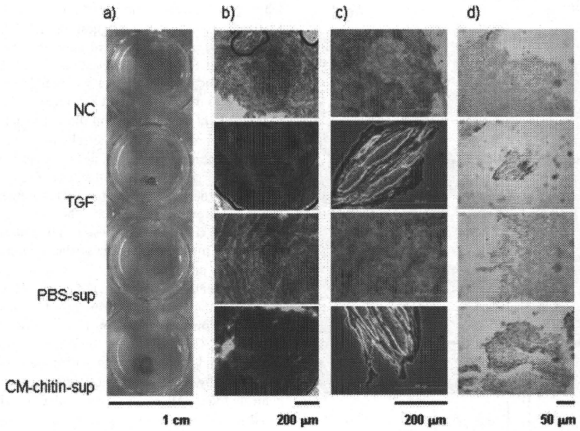

FIGURE 5. Histological evaluation of micromass tissues. (a) Alcian blue staining of tissues on day 21, observed at low magnification. (b) Alcian blue staining of tissues on day 21, observed at high magnification. (c) Toluidine blue staining of tissues on day 28. Tissues containing acidic glycosaminoglycan were stained a deep magenta color. (d) Immunohistological staining of tissues on day 28 with anti-collagen II antibody. Tissues containing collagen II were stained deep brown. In Figures (c and d), samples of TGF-β1 medium (TGF) and CM-chitin conditioned medium (CM-chitin-sup) were paraffinized, sectioned (12 μm), and deparaffinized before staining, while nontreated (NC) and PBS-conditioned medium (PBS-sup) treated tissues were not subjected to sectioning. [Color figure can be viewed in the online issue, which is available at www.interscience.wiley.com.]

expression in the CM-chitin treated micromass culture did not. The differences in Col2a1, Comp, and Col1a1 expression between the CM-chitin–treated and TGF-β1–treated micromass cultures [Fig. 3(b,d,e)] were probably due to another factor secreted from PEC, but this remains to be elucidated. We also showed here that blocking the TGF-β1 signal with anti-TGF-β1 antibody inhibited the expression of chondrogenic markers [Fig. 4(a–c)]. This indicated that TGF-β1 is one of the most important factors for chondrogenesis in micromass culture using CM-chitin-sup.

It has also been shown in previous studies that Comp, cartilage-oligomeric-protein, binds to collagen types I and II in the ECM and facilitates their structural stability.[55,56] Although Comp is synthesized by chondrocytes, osteoblasts, tenocytes, and ligament cells *in vivo*,[57,58] it is also synthesized by several mesenchymal cell–derived chondrocytes *in vitro*.[49,59,60] It was also reported that several types of TGF-β promote the expression of Comp in chondrogenic tissue from MSC.[61] Our result, which showed enhancement of Comp expression in micromass tissue due to treatment with TGF-β1 or CM-chitin-sup, is consistent with this report.

Histological evaluation showed the induction of glycosaminoglycan and type II collagen in CM-chitin-sup–treated micromass tissue (Fig. 5). Furthermore, a specific aggregation pattern was observed in the micromass tissue [Fig. 5(a)]. It has been reported that the treatment of micromass cultures of C3H10T1/2 cells with TGF-β1 resulted in the formation of a 3D spheroid culture exhibiting cartilage-like histology.[28,30] The aggregation pattern of the CM-chitin-sup–treated micromass tissue closely resembled that of the TGF-β1–treated micromass tissue [Fig. 5(a)], suggesting that the factors secreted by cells stimulated by CM-chitin–induced chondrogenesis in micromass culture.

Our results obtained in the present and previous studies suggested that the stimulation of CM-chitin induces the secretion of TGF-β1 from immune cells and results in the promotion of chondrogenesis in micromass culture. This shows that CM-chitin plays dual roles in cartilage regeneration as a scaffold and growth factor inducer. Recently, Yasuda et al. developed a novel method for inducing spontaneous *in vivo* cartilage regeneration by implanting a double-network hydrogel material into osteochondral defects of the femoral joint.[62] They observed spontaneous *in vitro* and *in vivo* chondrogenesis using a functional polymeric compound. Here, we also observed spontaneous *in vitro* chondrogenesis with a CM-chitin polymer without using any additional growth factors. Although the mechanism of the induction of TGF-β1 production in immune cells treated with CM-chitin has not been clarified, the CM-chitin–based cartilage regeneration method is a good candidate for tissue engineering as it does not require growth factors.

References

1. Shapiro F, Koide S, Glimcher MJ. Cell origin and differentiation in the repair of full-thickness defects of articular cartilage. J Bone Joint Surg Am 1993;75:532–553.

2. Oka M. Biomechanics and repair of articular cartilage. J Orthop Sci 2001;6:448–456.
3. Ochi M, Adachi N, Nobuto H, Yanada S, Ito Y, Agung M. Articular cartilage repair using tissue engineering technique—Novel approach with minimally invasive procedure. Artif Organs 2004; 28:28–32.
4. Tuan RS, Boland G, Tuli R. Adult mesenchymal stem cells and cell-based tissue engineering. Arthritis Res Ther 2003;5:32–45.
5. Erggelet C, Steinwachs MR, Reichelt A. The operative treatment of full thickness cartilage defects in the knee joint with autologous chondrocyte transplantation. Saudi Med J 2000;21:715–721.
6. Kim UJ, Park J, Kim HJ, Wada M, Kaplan DL. Three-dimensional aqueous-derived biomaterial scaffolds from silk fibroin. Biomaterials 2005;26:2775–2785.
7. Wang Y, Kim UJ, Blasioli DJ, Kim HJ, Kaplan DL. In vitro cartilage tissue engineering with 3D porous aqueous-derived silk scaffolds and mesenchymal stem cells. Biomaterials 2005;26:7082–7094.
8. Lu L, Zhu X, Valenzuela RG, Currier BL, Yaszemski MJ. Biodegradable polymer scaffolds for cartilage tissue engineering. Clin Orthop Relat Res 2001;391:S251–S270.
9. Reinholz GG, Lu L, Saris DB, Yaszemski MJ, O'Driscoll SW. Animal models for cartilage reconstruction. Biomaterials 2004;25: 1511–1521.
10. Kimura T, Yasui N, Ohsawa S, Ono K. Chondrocytes embedded in collagen gels maintain cartilage phenotype during long-term cultures. Clin Orthop Relat Res 1984;186:231–239.
11. Chiroff RT, White RA, White EW, Weber JN, Roy D. The restoration of the articular surfaces overlying replamineform porous biomaterials. J Biomed Mater Res 1977;11:165–178.
12. Suominen E, Aho AJ, Vedel E, Kangasniemi I, Uusipaikka E, Yli-Urpo A. Subchondral bone and cartilage repair with bioactive glasses, hydroxyapatite, and hydroxyapatite-glass composite. J Biomed Mater Res 1996;32:543–551.
13. Cui JH, Park K, Park SR, Min BH. Effects of low-intensity ultrasound on chondrogenic differentiation of mesenchymal stem cells embedded in polyglycolic acid: An *in vivo* study. Tissue Eng 2006;12:75–82.
14. Lisignoli G, Cristino S, Piacentini A, Zini N, Noel D, Jorgensen C, Facchini A. Chondrogenic differentiation of murine and human mesenchymal stromal cells in a hyaluronic acid scaffold: Differences in gene expression and cell morphology. J Biomed Mater Res A 2006;77:497–506.
15. Banu N, Tsuchiya T. Markedly different effects of hyaluronic acid and chondroitin sulfate-A on the differentiation of human articular chondrocytes in micromass and 3-D honeycomb rotation cultures. J Biomed Mater Res A 2007;80:257–267.
16. Wozney JM, Rosen V, Celeste AJ, Mitsock LM, Whitters MJ, Kriz JM, Hewick RM, Wang EA. Novel regulators of bone formation: Molecular clones and activities. Science 1988;242:1528–1534.
17. Rosen V, Wozney JM, Wang EA, Cordes P, Celeste A, McQuaid D, Kurtzberg L. Purification and molecular cloning of a novel group of BMPs and localization of BMP mRNA in developing bone. Conn Tiss Res 1989;20:313–319.
18. Celeste AJ, Iannazzi JA, Taylor RC, Hewick RM, Rosen V, Wang EA, Wozney JM. Identification of transforming growth factor β family members present in bone-inductive protein purified from bovine bone. Proc Natl Acad Sci USA 1990;87:9843–9847.
19. Centrella M, Horowitz MC, Wozney JM, McCarthy TL. Transforming growth factor-β gene family members and bone. Endocrine Rev 1994;15:27–39.
20. Denker AE, Haas AR, Nicoll SB, Tuan RS. Chondrogenic differentiation of murine C3H10T1/2 multipotential mesenchymal cells: I. Stimulation by bone morphogenetic protein-2 in high-density micromass cultures. Differentiation 1999;64:67–76.
21. Li WJ, Tuli R, Okafor C, Derfoul A, Danielson KG, Hall DJ, Tuan RS. A three-dimensional nanofibrous scaffold for cartilage tissue engineering using human mesenchymal stem cells. Biomaterials 2005;26:599–609.
22. Masuda S, Yoshihara Y, Muramatsu K, Wakebe I. Repairing of osteochondral defects in joint using β-TCP / carboxymethyl chitin composite. Key Eng Mater 2005;284:791–794.
23. Kariya H, Kiyohara A, Masuda S, Yoshihara Y, Ueno M, Hashimoto M, Suda Y. Biological roles of carboxymetyl-chitin associated for the growth factor production. J Biomed Mater Res A 2007:83:58–63.
24. Shi Y, Massague J. Mechanisms of TGF-beta signaling from cell membrane to the nucleus. Cell 2003;113:685–700.
25. Newman SA. Lineage and pattern in the developing vertebrate limb. Trends Clenet 1988;4:329–332.
26. Hall BK, Miyake T. The membranous skeleton: The role of cell condensations in vertebrate skeletogenesis. Annt Embryol (Berl) 1992;186:107–124.
27. Zhang X, Ziran N, Gouter JJ, Sehwarz EM, Puzas JE, Rosier RN, Zuscik M, Drissi H, O'Keefe RJ. Primary murine limb bud mescenchymal cells in long-term culture complete chondrocyte differentiation: TGF-beta Delays hypertrophy and PGE2 inhibits terminal differentiation. Bone 2004;34:809–817.
28. Denker AE, Nicoll SB, Tuan RS. Formation of cartilage-like spheroids by micromass cultures of murine C3H10T1/2 cells upon treatment with transforming growth factor-beta 1. Differentiation 1995;59:25–34.
29. Haas AR, Tuan RS. Chondrogenic differentiation of murine C3H10T1/2 multipotential mesenchymal cells: II. Stimulation by bone morphogenetic protein-2 requires modulation of N-cadherin expression and function. Differentiation 1999;64:77–89.
30. Song JJ, Aswad R, Kanaan RA, Rico MC, Owen TA, Barbe MF, Safadi FF, Popoff SN. Connective tissue growth factor (CTGF) acts as a downstream mediator of TGF-beta1 to induce mesenchymal cell condensation. J Cell Physiol 2007;210:398–410.
31. Tokura S, Nishi N, Tsutsumi A, Somorin O. Studies on chitin VIII. Some properties of water soluble chitin Derivatives. Polym J 1983;15:485–489.
32. Ahrens M, Ankenbauer T, Schroder D, Hollnagel A, Mayer H, Gross G. Expression of human bone morphogenetic protein-2 or 4 in murine mesenchymal progenitor cells induces differentiation into distinct mesenchymal cell lineages. DNA Cell Biol 1993;12: 871–880.
33. Rosenberq L. Chemical basis for the histological use of safranin O in the study of articular cartilage. J Bone Joint Surg Am 1971;53: 69–82.
34. van Sliedregt A, van Blitterswijk CA, Hesseling SC, Grote JJ, dcGroot K. The effect of the molecular weight of polylactic acid on *in vitro* biocompatibility. Adv Biomater 1990;9:207–212.
35. Athanasion KA, Niederauer GG, Agrawal CM. Sterilization, toxicity, biocompatibility and clinical applications of polylactic acid/ polyglycolic acid copolymers. Biomaterials 1996;17:93–102.
36. Freed LE, Marquis JC, Nohria A, Emmanual J, Mikos AG, Langer R. Neocartilage formation *in vitro* and *in vivo* using cells cultured on synthetic biodegradable polymers. J Biomed Mater Res 1993; 27:11–23.
37. Meinel L, Hofmann S, Karageorgiou V, Kirker-Head C, McCool J, Gronowicz G, Zichner L, Langer R, Vunjak-Novakovic G, Kaplan DL. The inflammatory responses to silk films *in vitro* and *in vivo*. Biomaterials 2005;26:147–155.
38. Li H, Schwartz NB. Gene structure of chick cartilage chondroitin sulfate proteoglycan (aggrecan) core protein. J Mol Evol 1995;41: 878–885.
39. Watanabe H, Yamada Y, Kimata K. Roles of aggrecan, a large chondroitin sulfate proteoglycan, in cartilage structure and function. J Biochem 1998;124:687–693.
40. Sekiya I, Tsuji K, Koopman P, Watanabe H, Yamada Y, Shinomiya K, Nifuji A, Noda M. SOX9 enhances aggrecan gene promoter/ enhancer activity and is up-regulated by retinoic acid in a cartilage-derived cell line, TC6. J Biol Chem 2000;275: 10738–10744.
41. Bayliss MT, Howat S, Davidson C, Dudhia J. The organization of aggrecan in human articular cartilage. Evidence for age-related changes in the rate of aggregation of newly synthesized molecules. J Biol Chem 2000;275:6321–6327.
42. Roark EF, Greer K. Transforming growth factor-beta and bone morphogenetic protein-2 act by distinct mechanisms to promote chick limb cartilage differentiation *in vitro*. Dev Dyn 1994;200: 103–116.
43. Watanabe H, de Caestecker MP, Yamada Y. Transcriptional cross-talk between Smad, ERK1/2, and p38 mitogen-activated protein kinase patyways regulates transforming growth factor-beta-induced

aggrecan gene expression in chondrogenic ATDC5 cells. J Biol Chem 2001;276:14466–14473.
44. Schmitt B, Ringe J, Haupl T, Notter M, Manz R, Burmester G-R, Sittinger M, Kaps C. BMP2 initiates chondrogenic lineage development of adult human mesenchymal stem cells in high-density culture. Differentiation 2003;71:567–577.
45. Tanaka H, Murphy CL, Murphy C, Kimura M, Kawai S, Polak JM. Chondrognic differentiation of murine embryonic stem cells: effects of culture conditions and dexamethasone. J Cell Biochem 2004;93:454–462.
46. zur Nieden NI, Kempka G, Rancourt DE, Ahr HJ. Induction of chondro-, osteo-, and adipogenesis in embryonic stem cells by bone morphogenetic protein-2: Effect of cofactors on differentiating lineages. BMC Dev Biol 2005;5:1
47. Tuli R, Tuli S, Nandi S, Huang X, Manner PA, Hozack W, Danielson KG, Hall DJ, Tuan RS. Transforming growth factor-β-mediated chondrogenesis of human mesenchymal progenitor cells involves N-cadherin and mitogen-activated protein kinase and Wnt signaling cross-talk. J Biol Chem 2003;278:41227–41236.
48. Lefebvre V, Huanq W, Harlev VR, Goodfellow PN, de Crombruqqhe B. Sox9 is a potent activator of the chondrocyte-specific enhancer of the pro alpha1(II) collagen gene. Mol Cell Biol 1997; 17:2336–2346.
49. Kulyk WM, Franklin JL, Hoffman LM. Sox9 expression during chondrogenesis in micromass cultures of embryonic limb mesenchyme. Exp Cell Res 2000;255:327–332.
50. Aszodi A, Hunziker EB, Olsen BR, Fassler R. The role of collagen II and cartilage fibril-associated molecules in skeletal development. Osteoarthritis Cartilage 2001;9:150–159.
51. Gustafsson E, Aszdi A, Orteqa N, Hunziker EB, Denker HW, Werb Z, Fassler R. Role of collagen type II and perlecan in skeletal development. Ann N Y Acad Sci 2003;995:140–150.
52. Bosnakovski D, Mizuno M, Kim G, Takaqi S, Okumura M, Fujinaqa T. Chondrogenic differentiation of bovine bone marrow mexenchymal stem cells (MSCs) in different hydrogels: Influence of collagen type II extracellular matrix on MSC chondrogenesis. Biotechnol Bioeng 2006;93:1152–1163.
53. Williams CG, Kim TK, Taboas A, Manson P, Elisseeff J. In vitro chondrogenesis of bone marrow-derived mesenchymal stem cells in a photopolymerizing hydrogel. Tissue Eng 2003;9:679–688.
54. Huang JI, Zuk PA, Jones NF, Zhu M, Lorenz HP, Hedrick MH, Benhaim P. Chondrogenic potential of multipotential cells from human adipose tissue. Plast Reconstr Surg 2004;113:585–594.
55. Hedbom E, Antonsson P, Hierpe A, Aeschimann D, Paulsson M, Rosa-Pimentel E, Sommarin Y, Wendel M, Oldberg A, Heinegard D. Cartilage matrix proteins. An acidic oligomeric protein (COMP) detected only in cartilage. J Biol Chem 1992;267:6132–6136.
56. Halasz K, Kassner A, Morqelin M, Heineqard D. COMP acts as a catalyst in collagen fibrillogenesis. J Biol Chem 2007;282: 31166–31173.
57. Kipnes J, Carlberg AL, Loredo GA, Lawler J, Tuan RS, Hall DJ. Effect of cartilage oligomeric matrix protein on mesenchymal chondrogenesis *in vitro*. Osteoarthritis Cartilage 2003;11:442–454.
58. Liu CJ, Prazak L, Fajardo M, Yu S, Tyagi N, Di Cesare PE. Leukemia/lymphoma-related factor, a POZ domain-containing transcriptional repressor, interacts with histone deacetylase-1 and inhibits cartilage oligomeric matrix protein gene expression and chondrogenesis. J Biol Chem 2004;279:47081–47091.
59. Chen AL, Frang C, Liu C, Leslie MP, Chang E, Di Cesare PE. Expression of bone morphogenetic proteins, receptors, and tissue inhibitors in human fetal, adult, and osteoarthritic articular cartilage. J Orthop Res 2004;22:1188–1192.
60. Im GI, J NH, Tae SK. Chondrogenic differentiation of mesenchymal stem cells isolated from patients in late adulthood: The optimal conditions of growth factors. Tissue Eng 2006;12:527–536.
61. Mehlhorn AT, Schmal H, Kaiser S, Lepski G, Finkenzeller G, Stark GB, Sudkamp NP. Mesenchymal stem cells maintain TGF-beta-mediated chondrogenic phenotype in alginate bead culture. Tissue Eng 2006;12:1393–1403.
62. K Yasuda, N Kitamura, JP Gong, K Arakaki, HJ Kwon, S Onodera, YM Chen, T Kurokawa, F Kanayam, Y Ohmiya, Y Osada. A novel double-network hydrogel induces spontaneous articular cartilage regeneration *in vivo* in a large osteochondral defect. Macromol Biosci 2009;9:307–316.